University of Zurich[UZH]

Lecture 1: Principles of direct dark matter detection

ISAPP 2024: Particle Candidates for Dark Matter
Scuola Galileiana di Studi Superiori
Padova, July 2, 2024

Laura Baudis
University of Zurich

Content

- Overview: DM candidates
- Direct detection: general remarks
- Astrophysics and the Standard Halo Model
- Kinematics
- The differential scattering rate
- Cross section predictions from particle physics
- SI and SD scattering, form factors
- Light DM detection

Dark matter candidates: overview

Lectures: Joerg Jaeckel, Igor Istaroza

$10^{-22}\,\mathrm{eV}$ QCD axion $1\,\mathrm{keV}$ $1\,\mathrm{GeV}$ $100\,\mathrm{TeV}$ M_{pl} $10\,M_\odot$

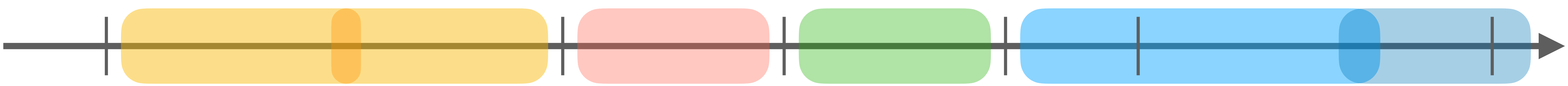

Ultra-light DM

bosonic fields

Light DM

dark sector

WIMP

Composite DM

Q-balls, dark atoms, dark mesons etc

PBHs

Structures on the scale of dwarf galaxies can form: $\lambda = \dfrac{2\pi}{mv} \sim \mathrm{kpc}$

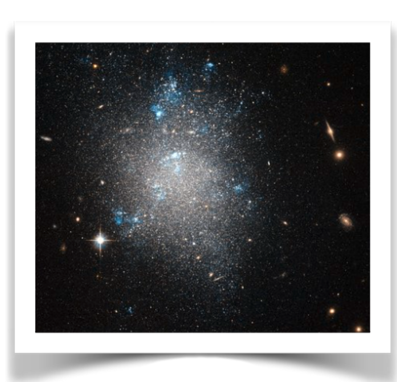

Credit: ESA/Hubble & NASA

weak scale dark matter

Lectures: Laura Covi

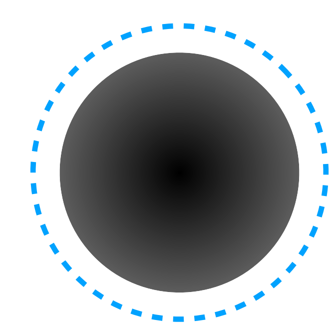

Direct detection: overview

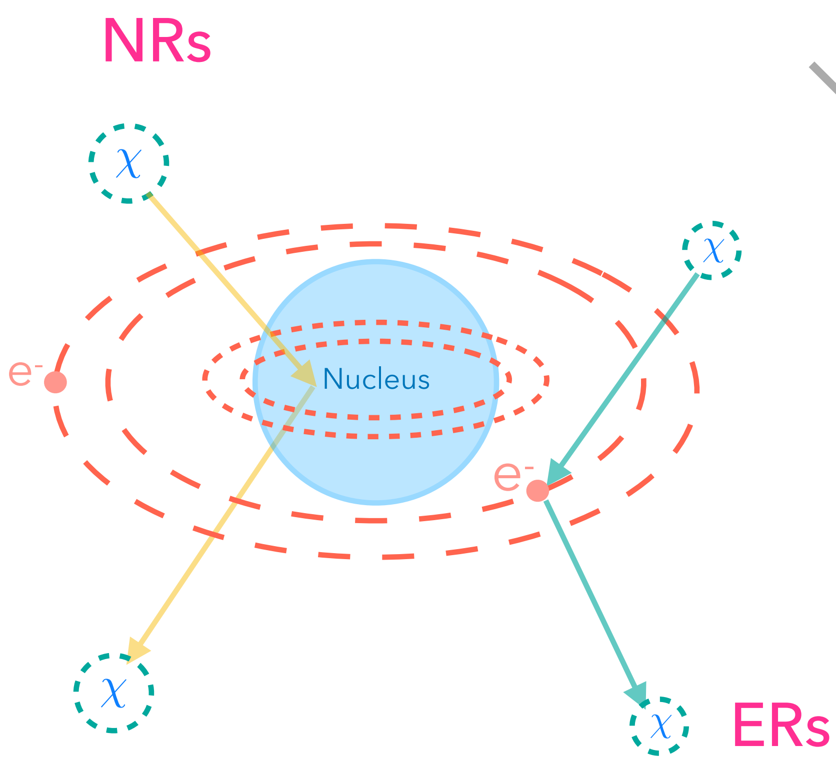

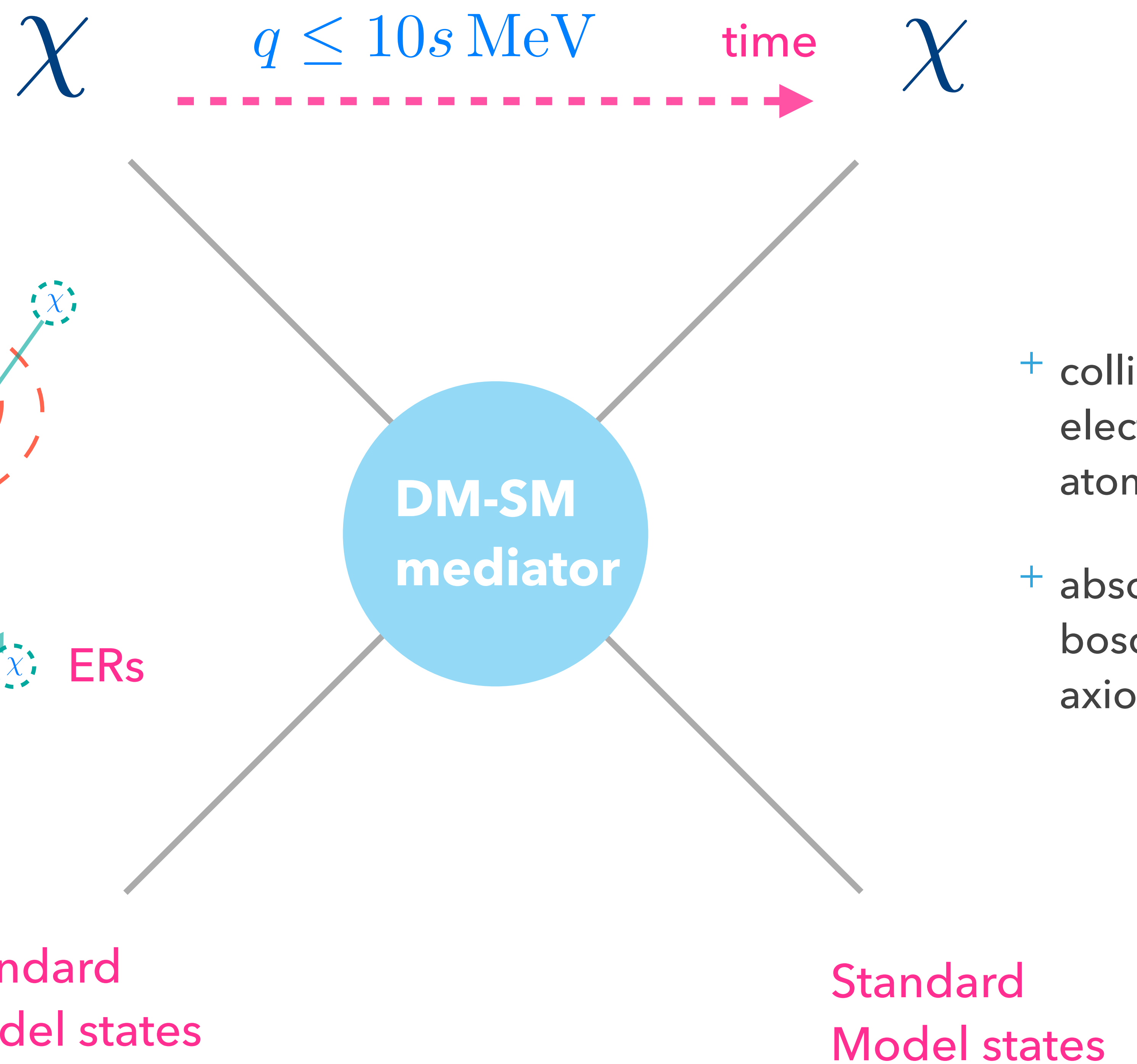

- collisions with electrons in the atomic shell,
- absorption of light bosons via, e.g., the axio-electric effect

Direct detection: overview

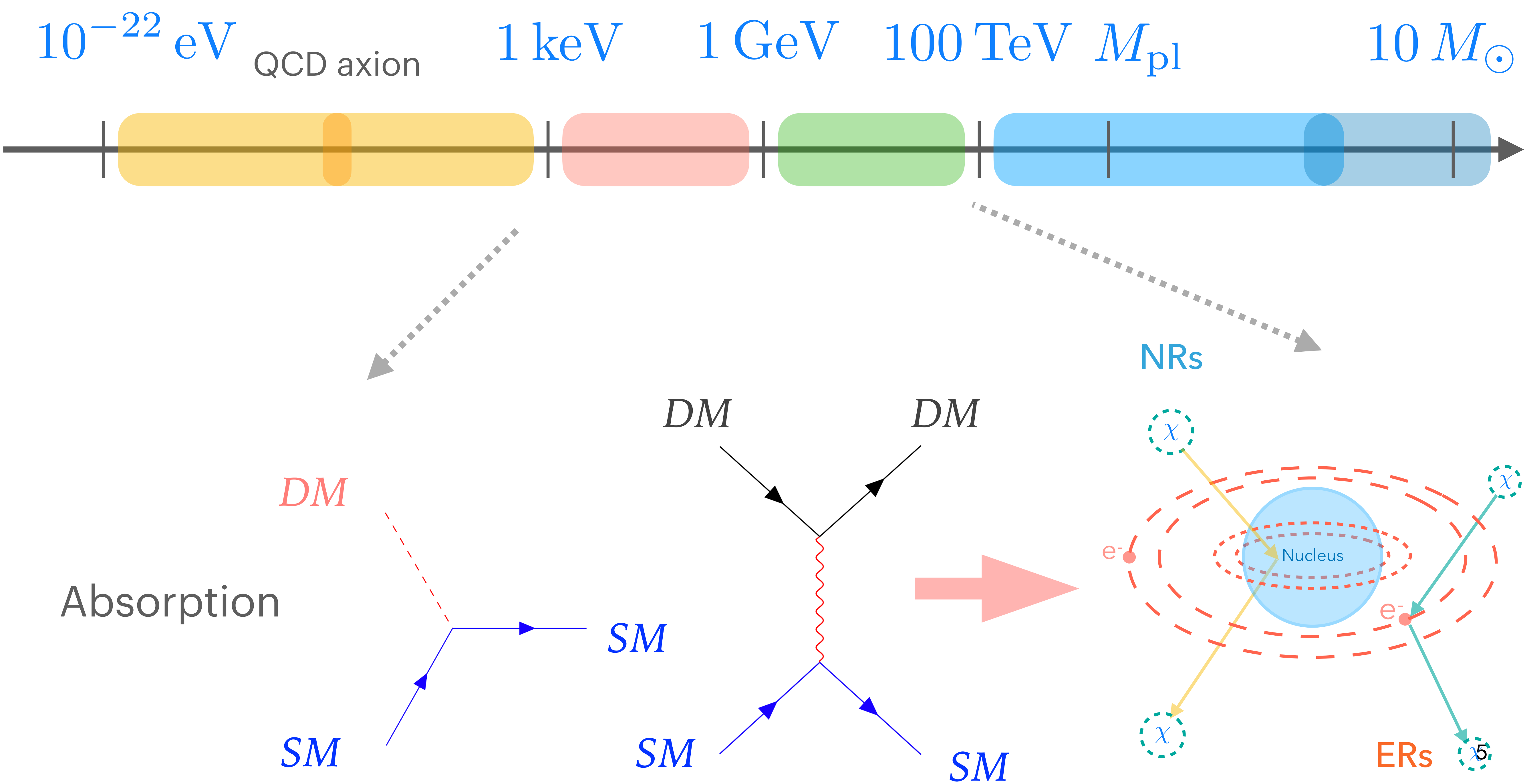

Direct detection: general remarks

- Search for scatters of galactic dark matter particles in terrestrial, deep underground detectors

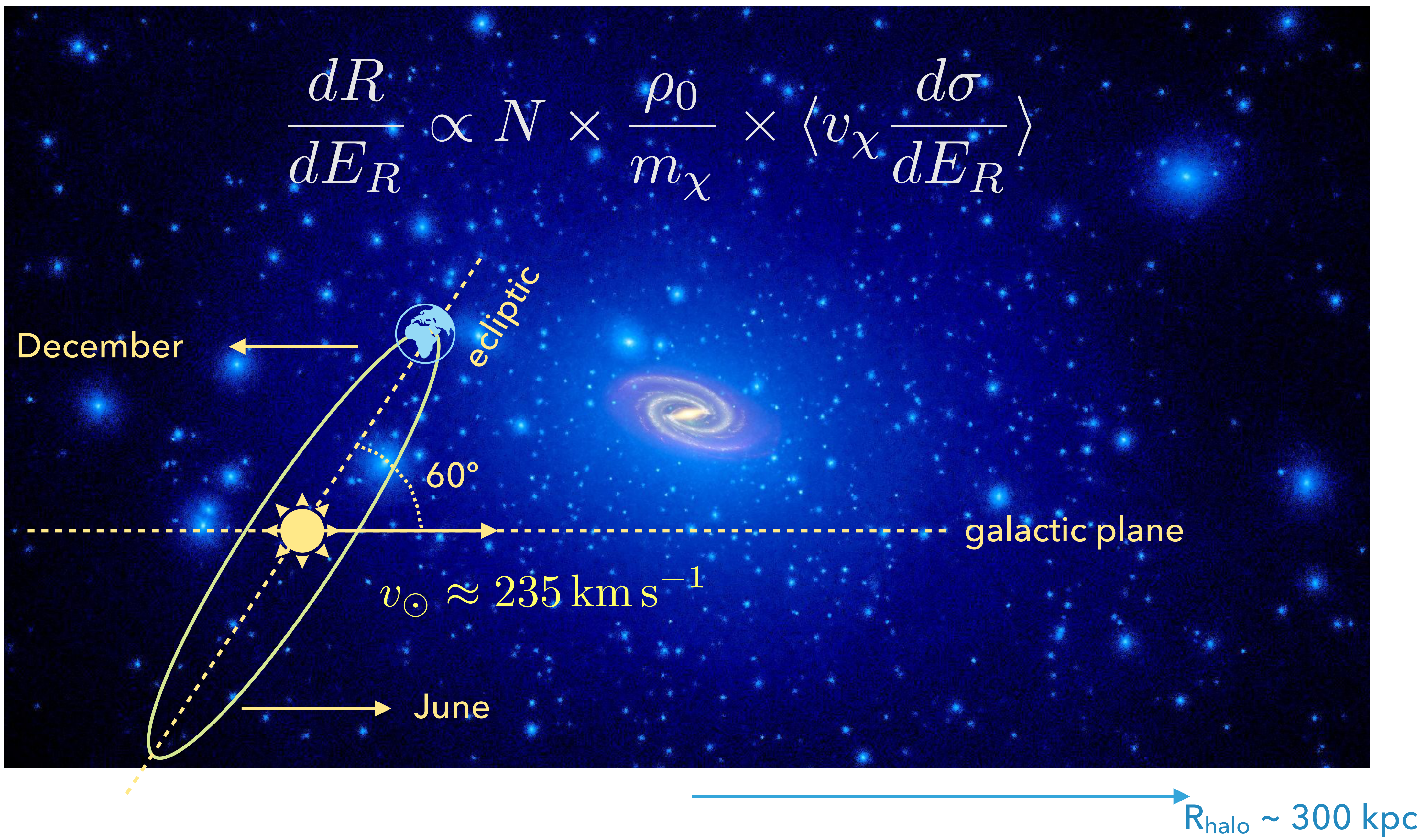

Direct detection: general remarks

- Main physical observable: a differential recoil spectrum
- Its modelling relies on inputs/tools from several fields!

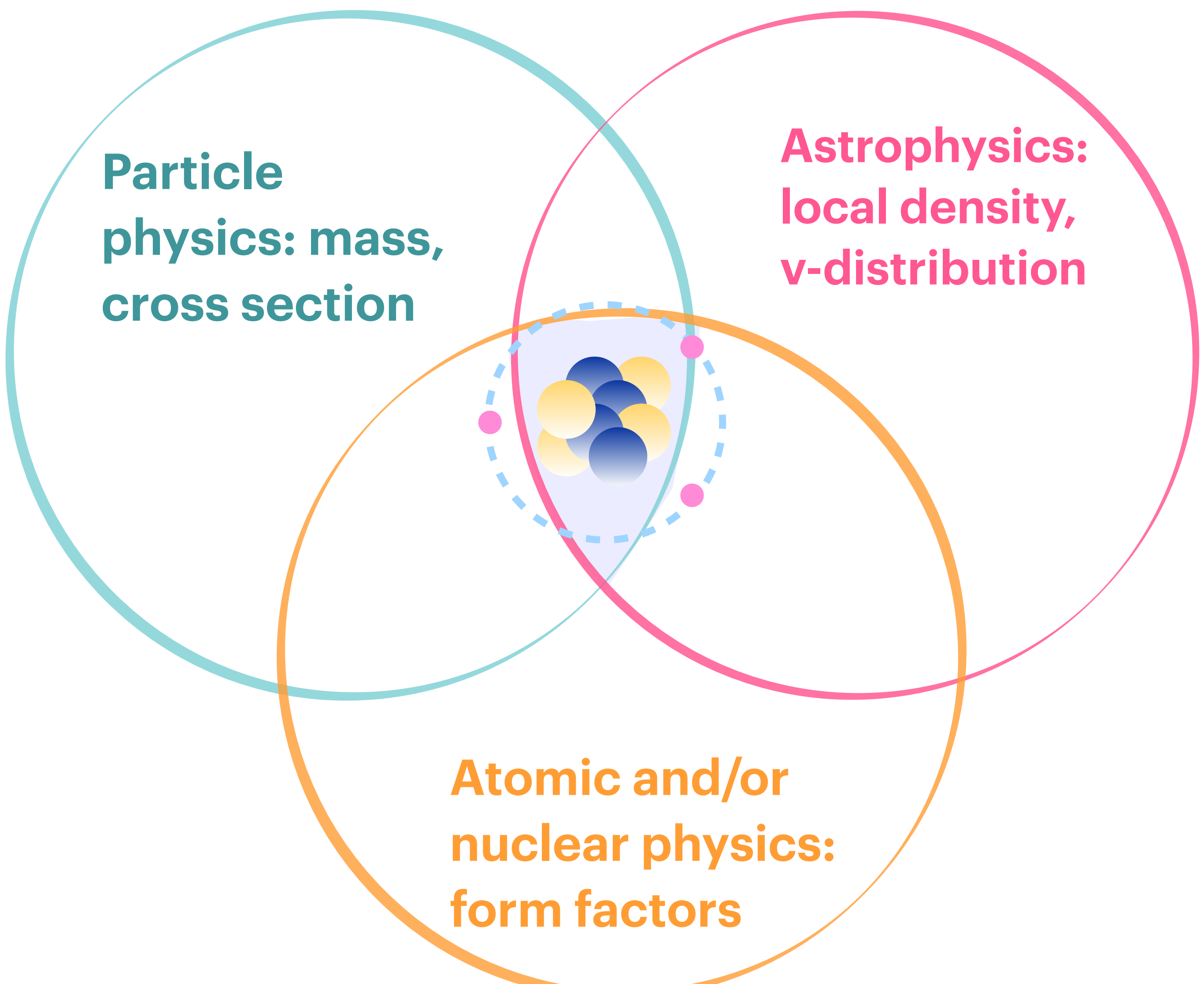

Overview: local DM density

- **Local measures**: vertical kinematics of stars near Sun as 'tracers' (smaller error bars, stronger assumptions about the halo shape)
- **Global measures**: extrapolate the density from Milky Way's rotation curve derived from kinematic measurements of gas, stars… (larger errors, fewer assumptions)

Major source of uncertainty: contribution of baryons (stars, gas, stellar remnants, …) to the local dynamical mass

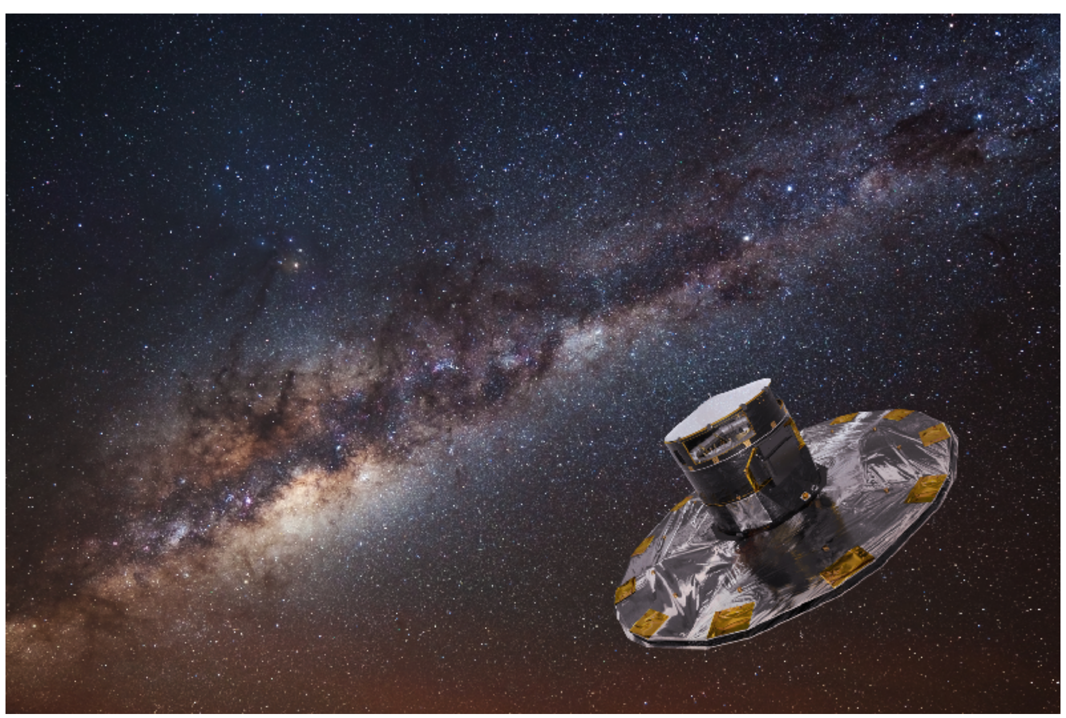

Gaia: positions, parallaxes, and proper motions for 2.5 x 10^9 stars

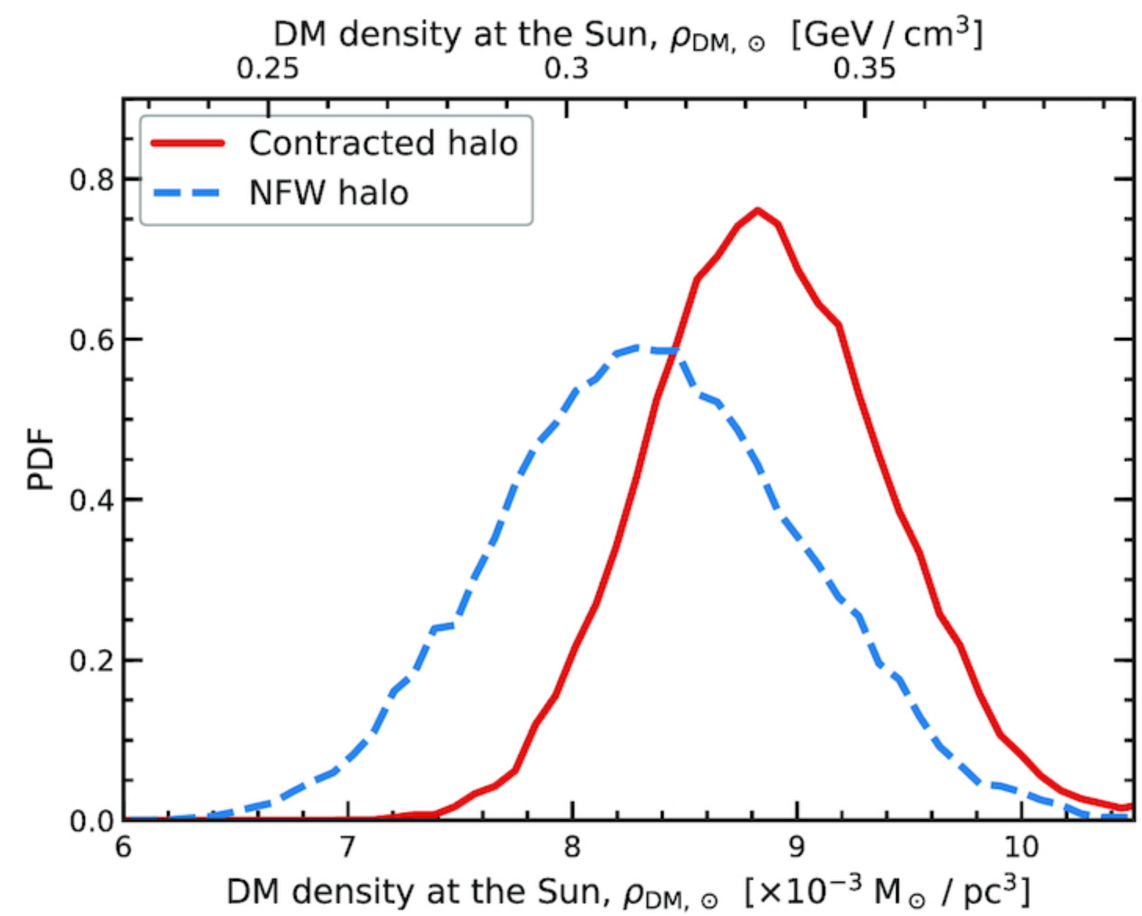

M. Cautun et al, MNRAS 494 (2020) 3, using Gaia DR2

Overview: local DM density

- **Local measures:** vertical kinematics of stars near Sun as 'tracers' (smaller error bars, stronger assumptions

Major source of uncertainty:

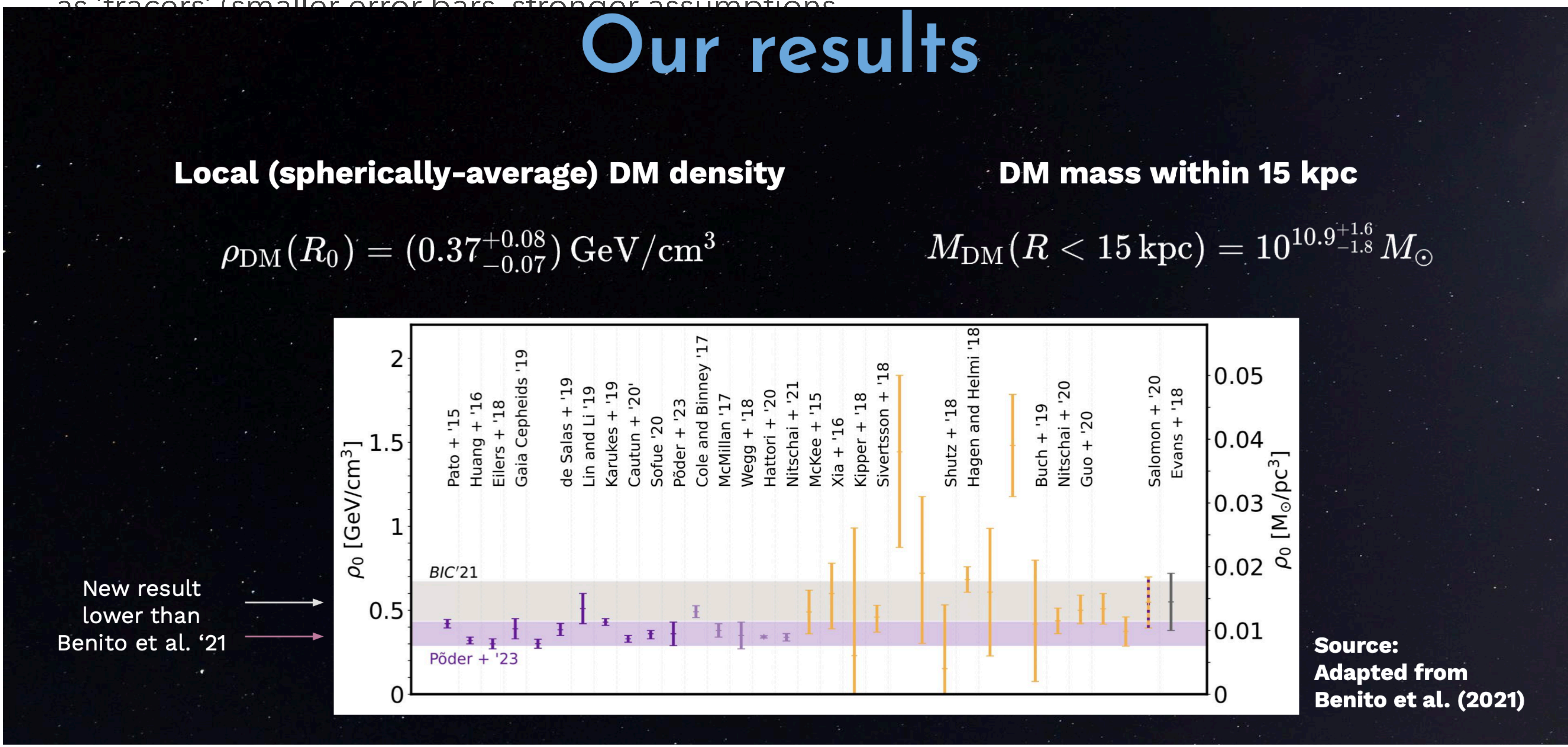

Sven Poder, Tartu Observatoorium; Talk at EuCAPPT, CERN, May 31, 2023

Overview: DM velocity distribution

- Standard halo model: Maxwellian distribution (isotropic velocities)

$$\rho(r) \propto r^{-2}$$

- Goal: determine f(v) from observation (e.g., motion of stars that share kinematics with DM)
- Recent studies: some deviations from SHM, due to anisotropies in the local stellar distribution (in Gaia data)
- These arise from accretion events, where the "Gaia-sausage" seems to be a dominant merger in the solar neighbourhood
- Effects for direct detection experiments: relevant mostly at low dark matter masses

Necib, Lissanti, Belorukov 2018, Evans, O'Hare, McCabe, PRD99, 2019; Buch, Fan, Leung, PRD101, 2020; and others

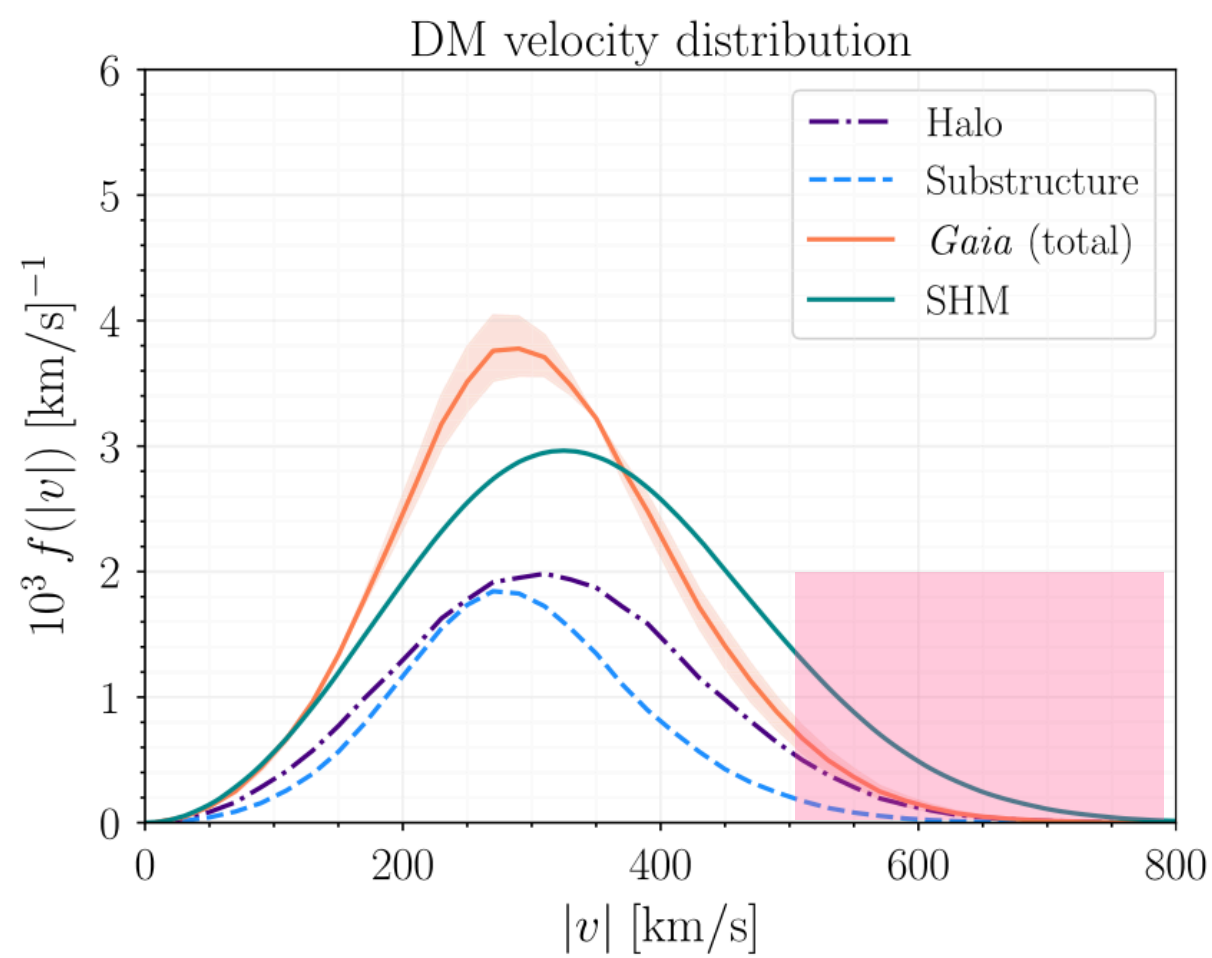

Normalised Gaia DM velocity distribution in heliocentric frame

Milky Way: fits to the observed rotation curve

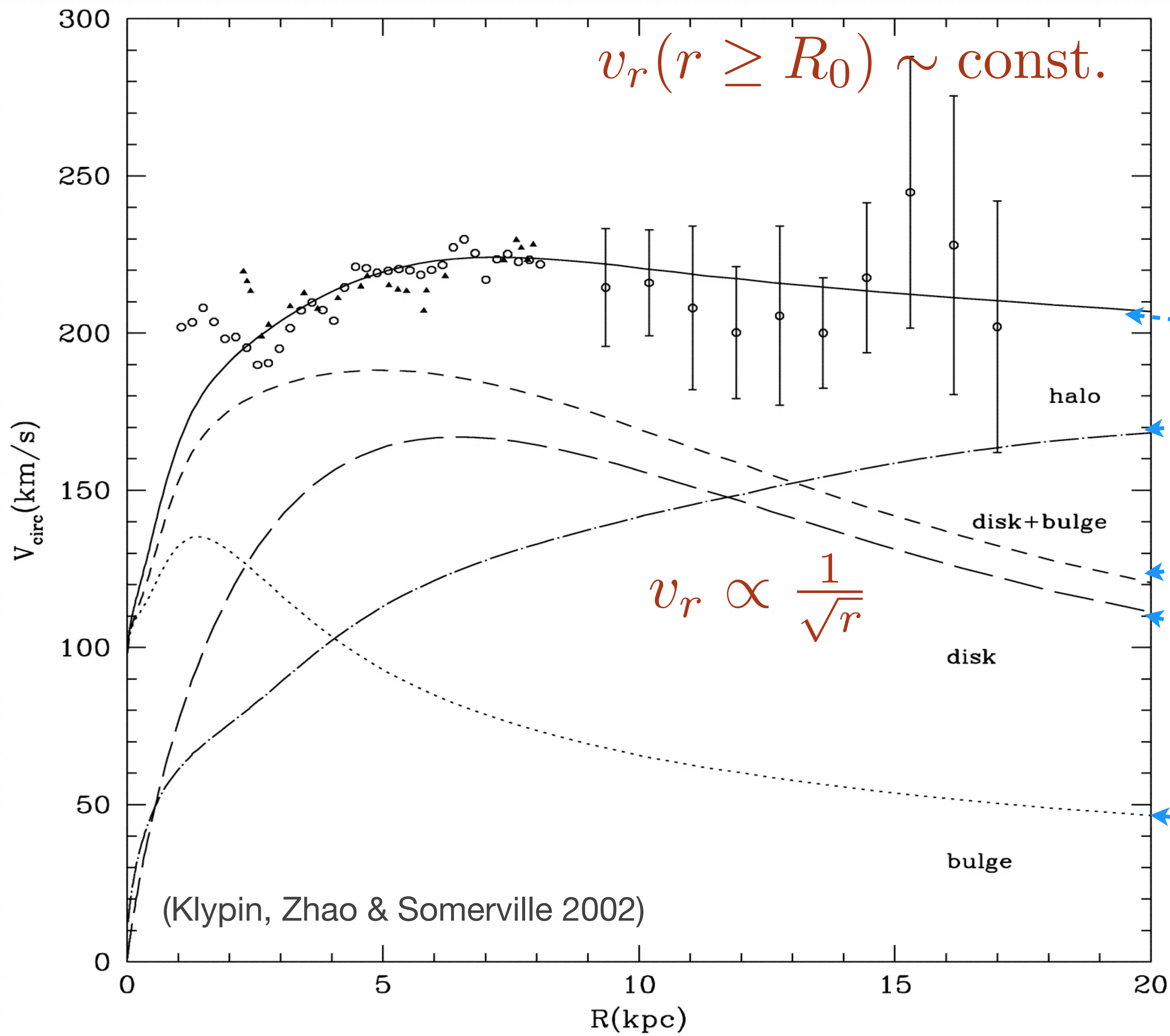

$\Longrightarrow M_r \propto r$

Sum of halo + disk + bulge

Dark matter halo

Disk + Bulge

Disk

Bulge

$M_{230\,\mathrm{kpc}} \approx 1.3 \times 10^{12} M_\odot$

$M_{\mathrm{tot,lum}} \approx 9 \times 10^{10} M_\odot$ $M_{25\,\mathrm{kpc}} \approx 2.8 \times 10^{11} M_\odot$

Rotation curve for different MV mass models

Iocco, Pato, Bertone, Jetzer, JCAP11, 2011

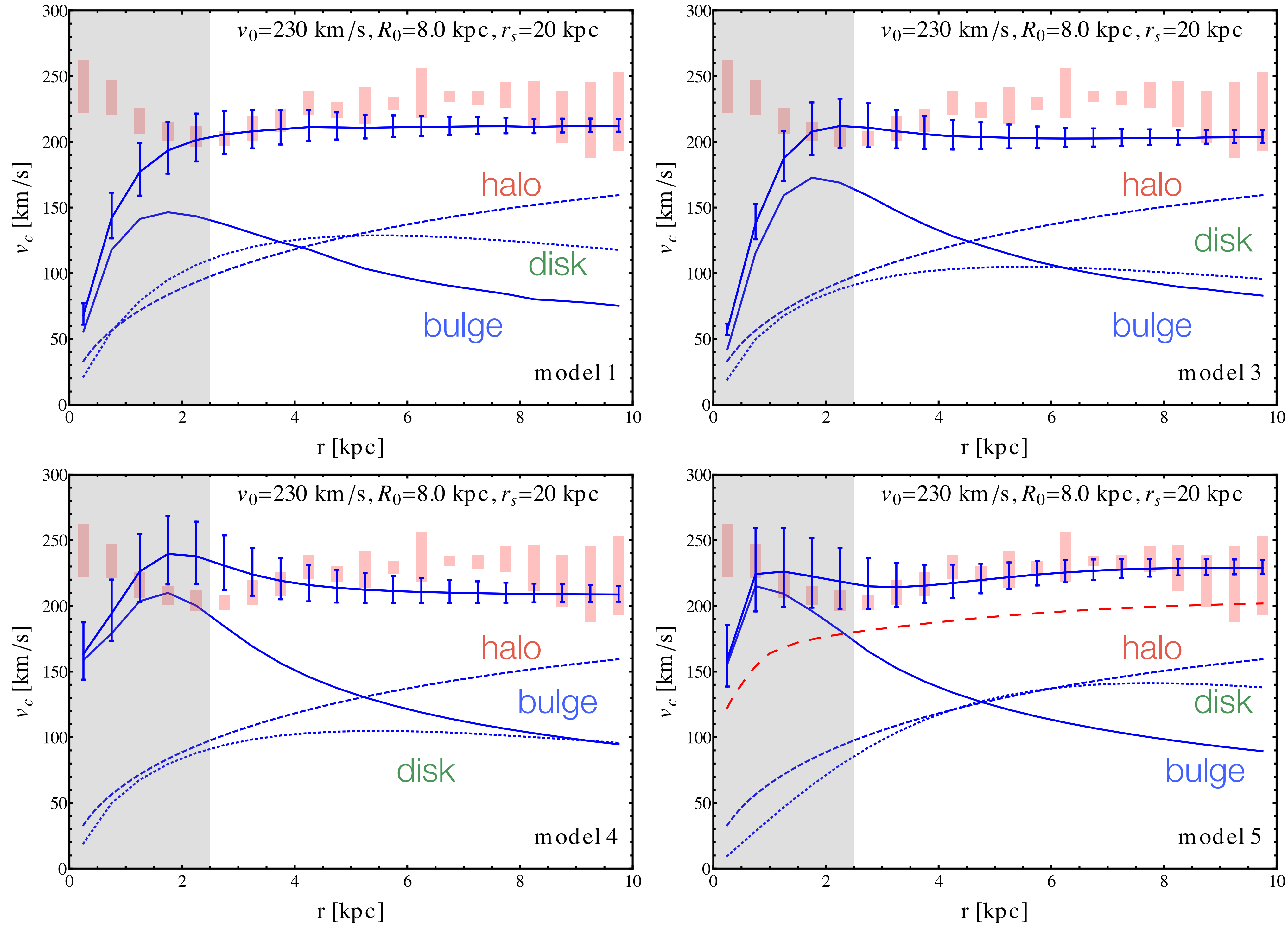

Galactic Rotation Curve

- Expectations: from centrifugal force = gravitational attraction (M$_r$ = total mass interior to r)

$$\frac{mv^2}{r} = G\frac{M_r m}{r^2}$$

$$v_r^2 = G\frac{M_r}{r}$$

$$v_r = \sqrt{\frac{GM_r}{r}}$$

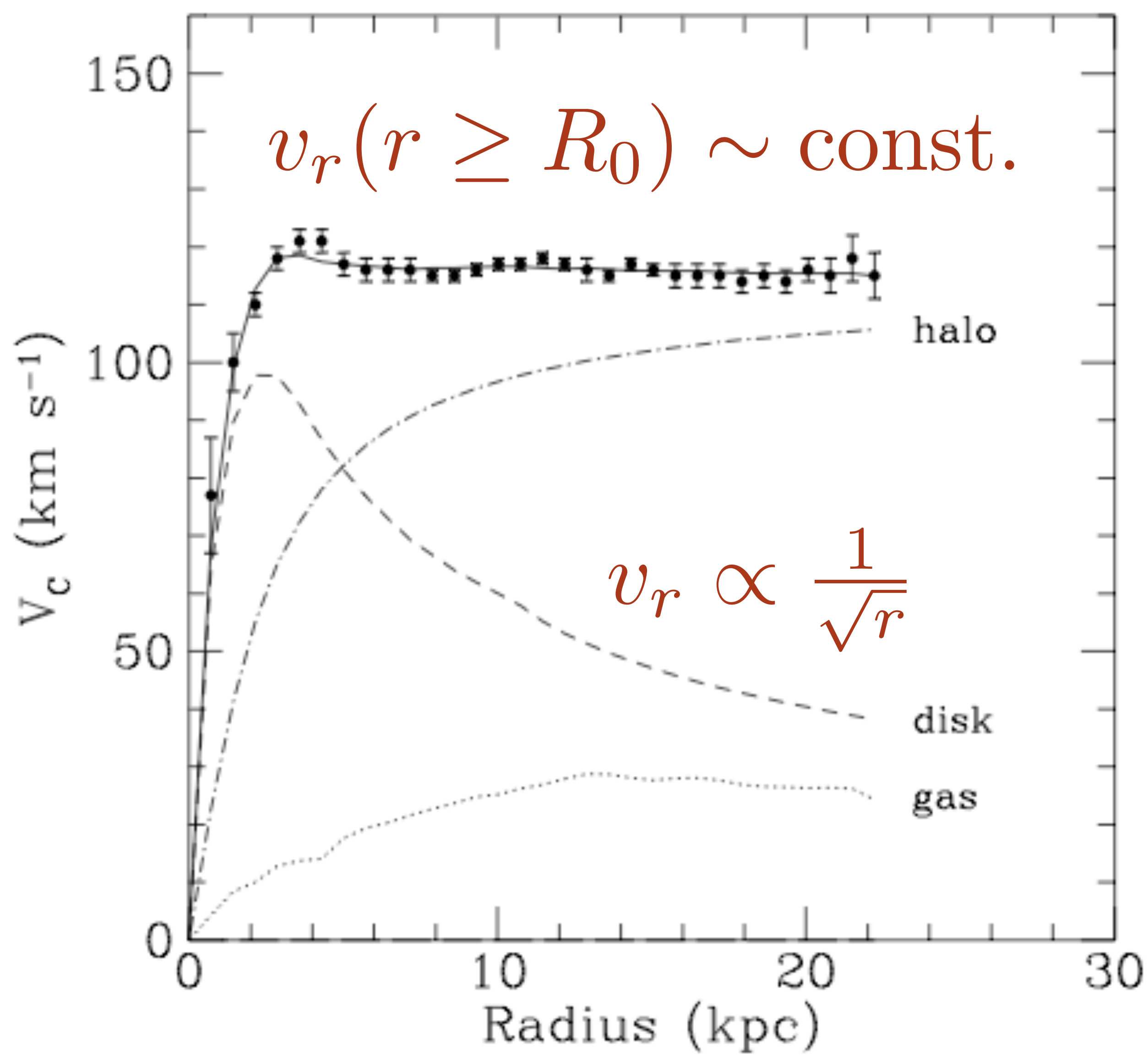

- Observations:

$$v_r(r \geq R_0) \approx \text{const.}$$

$$\Longrightarrow M_r \propto r$$

⇒ a non-visible mass component, which increases linearly with radius, must exist

Galactic Rotation Curve

- **The rotation curve depends on the distribution of mass** ⇒ one can thus use the measured rotation curve to learn about the dark matter distribution

  "Rigid body" rotation: the mass must be ~ spherically distributed and the density ρ ~ constant

  Flat rotation curve: most of the matter in the outer parts of the galaxy is spherically distributed, and the density is

$$\rho(r) \propto r^{-2}$$

- To see this, we assume a constant rotation velocity V. *The force, acting on a star of mass m by the mass M_r of the galaxy inside the star's position r is:*

$$\frac{mV^2}{r} = G\frac{M_r m}{r^2}$$

- if we assume spherical symmetry. We solve for M_r:

$$M_r = \frac{V^2 r}{G}$$

- and then differentiate with respect to the radius r of the distribution:

$$\frac{dM_r}{dr} = \frac{V^2}{G}$$

Galactic Rotation Curve

- We then use the equation for the conservation of mass in a spherically symmetric system:

$$\frac{dM_r}{dr} = 4\pi r^2 \rho(r)$$

- and obtain for the **mass density in the outer parts of the Milky Way**:

$$\rho(r) = \frac{V^2}{4\pi r^2 G}$$

- The $1/r^2$-dependency is in strong contrast to the number density of stars in the visible, stellar halo, which varies with $1/r^{3.5}$, thus decays much more rapidly as one would expect from the galactic rotation curve
- this discrepancy came as a big surprise to astronomers

⇒ the main component of the Milky Way's mass is in a form non-luminous, or dark matter

[so far, the dark matter has been observed only indirectly, through its gravitational influence on visible matter]

Galactic Rotation Curve

- One needs however to modify the previous equation:

$$\rho(r) = \frac{V^2}{4\pi r^2 G}$$

- in order to force the density function to approach a constant value near the centre (rather than to diverge!), to be consistent with the **observational evidence of a rigid-body rotation**
- Thus, a better form for the density distribution is given by:

$$\rho(r) = \frac{C_0}{a^2 + r^2}$$

- where the parameters (C_0, a) are obtained from fits to the overall measured rotation curve, e.g.:

$$C_0 = 4.6 \times 10^8 M_{\odot} \mathrm{kpc}^{-1}$$

$$a = 2.8\,\mathrm{kpc}$$

We note that:

for r $\gg$ a $\Rightarrow$ $\rho(r) \propto r^{-2}$

for r $\ll$ a $\Rightarrow$ $\rho(r) \propto$ const.

The Standard Halo Model

- The standard halo model (SHM) is an isotropic, isothermal sphere with density profile r^{-2}. In this case, the solution of the collisionless Boltzmann equation is a so-called Maxwellian velocity distribution, given by:

$$f(\mathbf{v}) = N \exp\left(-\frac{3|\mathbf{v}|^2}{2\sigma^2}\right)$$

- where N is a normalisation constant. The velocity dispersion is related to the asymptotic value of the circular speed, which is the speed at which objects on circular orbits orbit the Galactic centre:

$$v_{\mathrm{c},\infty} = \sqrt{2/3}\,\sigma$$

- Usually it is assumed that the rotation curve has already reached its asymptotic value at the solar radius $r = R_0$, such that:

$$\sigma = \sqrt{3/2}\,v_{\mathrm{c}}$$

- where

$$v_{\mathrm{c}} \equiv v_{\mathrm{c}}(R_0)$$

The Standard Halo Model

- The density distribution in the SHM is formally infinite and hence the velocity distribution also extends to infinity. **In reality however, the Milky Way halo is finite, and particles with speeds greater than the escape speed:**

$$v_{\rm esc}(r) = \sqrt{2|\phi(r)|} \qquad\qquad \phi(r) \text{ is the potential}$$

will not be gravitationally bound to the Milky Way.

- This is addressed by truncating the velocity distribution at the measured local escape speed:

$$v_{\rm esc} \equiv v_{\rm esc}(R_0)$$

- such that

$$f(\mathbf{v}) = 0 \text{ for } |\mathbf{v}| \geq v_{\rm esc}$$

see, e.g. Anne M Green JoPG, 44 084001, 2017

- or (to make the truncation smooth):

$$f(\mathbf{v}) = \begin{cases} N\left[\exp\left(-\frac{3|\mathbf{v}|^2}{2\sigma^2}\right)\exp\left(-\frac{3v_{\rm esc}^2}{2\sigma^2}\right)\right], & |\mathbf{v}| < v_{\rm esc}\,, \\ 0\,, & |\mathbf{v}| \geq v_{\rm esc}\,. \end{cases}$$

The Standard Halo Model

- **The standard parameter values used for the SHM are the following:**

- local density

$$\rho_0 \equiv \rho(R_0) = 0.3\,\mathrm{GeV\,cm^{-3}}$$

$$\rho_0 = 0.008 M_\odot \mathrm{pc}^{-3} = 5\times 10^{-25}\mathrm{g\,cm^{-3}}$$

- local circular speed

$$v_\mathrm{c} = 220\,\mathrm{km\,s^{-1}}$$

- local escape speed

$$v_\mathrm{esc} = 544\,\mathrm{km\,s^{-1}}$$

- The escape speed is the speed required to escape the local gravitational field of the MW, and the local escape speed is estimated from the speeds of high velocity stars
- The RAVE survey had measured (later improved with SDSS and Gaia data):

$$498\,\mathrm{km\,s^{-1}} < v_{esc} < 608\,\mathrm{km\,s^{-1}}$$

Recommendations for DD experiments

See *EPJ-C* 81 (2021) 10, 907

- Community effort towards using the same astrophysical parameters in the analysis of direct detection experiments' data

Eur. Phys. J. C (2021) 81:907 Page 11 of 19 **907**

Table 1 Suggested Standard Halo Model parameters. Vectors are given as (v_r, v_ϕ, v_θ) with r pointing radially inward and ϕ in the direction of the Milky Way's rotation. Analyses insensitive to annular modulation can approximate $\mathbf{v}_\oplus(t)$ with Eq. 12

Parameter	Description	Value	References
ρ_χ	Local dark matter density	$0.3\text{GeV}/\text{c}^2/\text{cm}^3$	[9]
v_{esc}	Galactic escape speed	544 km/s	[45]
$\langle\lvert\mathbf{v}_\oplus\rvert\rangle$	Average galactocentric Earth speed	29.8 km/s	[41]
$\mathbf{v}_\circledast$	Solar peculiar velocity	(11.1, 12.2, 7.3) km/s	[46]
$\mathbf{v}_0$	Local standard of rest velocity	(0, 238, 0) km/s	[47,48]

Table 2 Reported values of galactic escape speed. The measurement reported in [70]* is a re-analysis of the data set using the same priors used in [71]

Year	References	Survey	Data release	C.L. (%)	v_{esc} interval (km/s)	v_{esc} median (km/s)
2007	[45]	RAVE	1 [68]	90	498–608	544
2014	[71]	RAVE	4 [72]	90	492–587	533
2017	[73]	SDSS	9 [74]	68	491–567	521
2018	[75]	*Gaia*	2 [50]	68	517–643	580
2019	[70]	*Gaia*	2 [50]	90	503–552	528
2019	[70]*	*Gaia*	2 [50]	90	548–612	580
2021	[76]	*Gaia*	2 [50]	68	477–502	485

Milky Way rotation curve

- A more recent compilation of all existing data

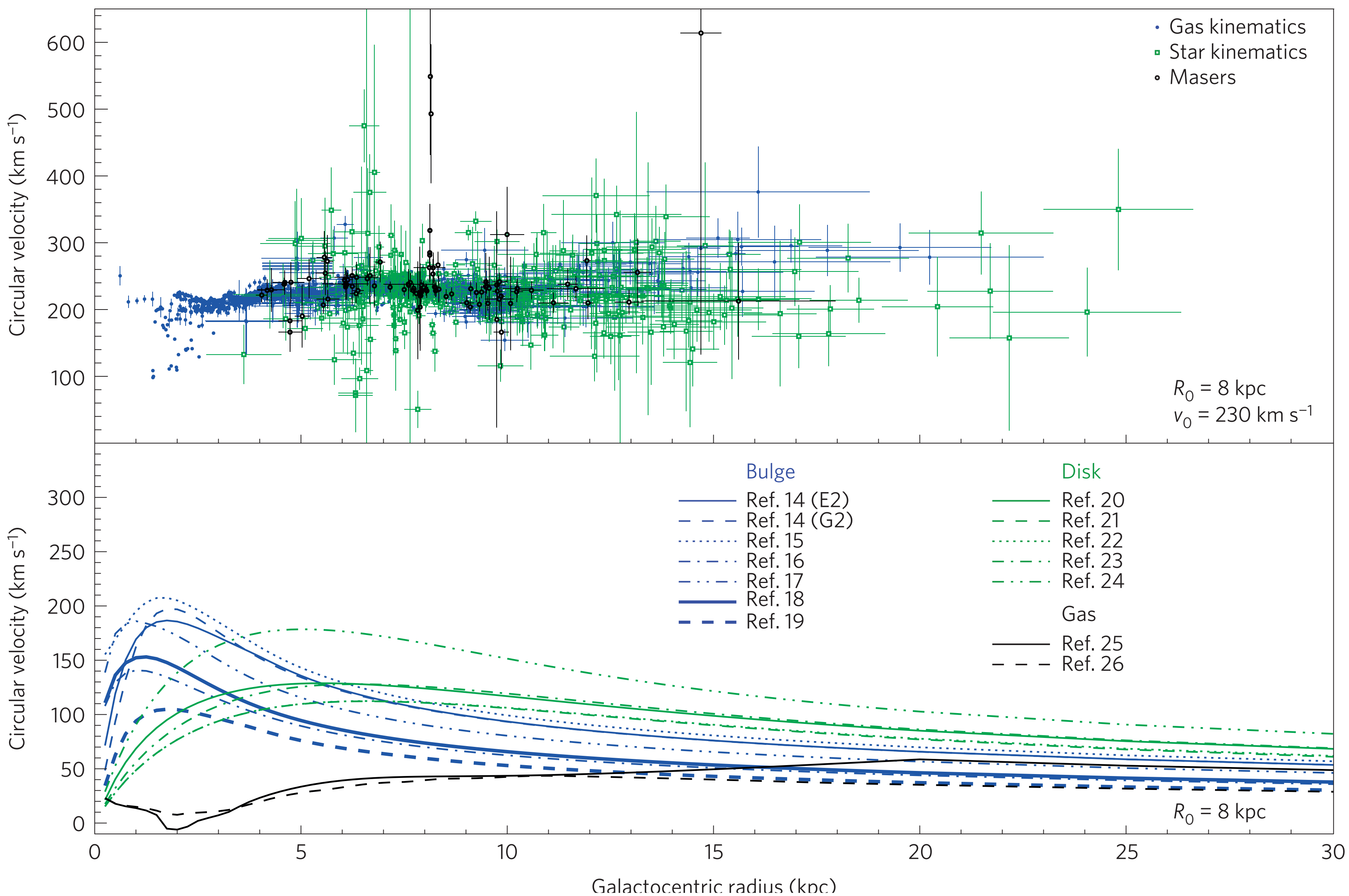

Rotation curve measurements (circular velocity as a function of galactocentric radius) including data from gas kinematics (HI, CO, HII regions, molecular clouds); star kinematics and masers

Contribution to the rotation curve as predicted from different models for the stellar bulge, stellar disk, and gas

F. Iocco, M. Pato, G. Bertone, Nature Physics, DOI 10.1038

Direct detection: DM flux on Earth

- For a typical WIMP mass of 100 GeV/c^2, the expected WIMP flux on Earth (for the 'standard local density' value) is:

$$\phi_\chi = \frac{\rho_\chi}{m_\chi} \times \langle v \rangle = 6.6 \times 10^4 \,\mathrm{cm}^{-2}\mathrm{s}^{-1}$$

- This flux is sufficiently large that, even though WIMPs are weakly interacting, a small but potentially measurable fraction will elastically scatter off nuclei in an Earth-bound detector
- Assuming a scattering cross section of 10^{-38} cm^2, the expected rate (for a nucleus with atomic mass A = 100) would be:

$$R = \frac{N_A}{A} \times \phi_\chi \times \sigma \sim 0.13\,\mathrm{events\,kg^{-1}yr^{-1}}$$

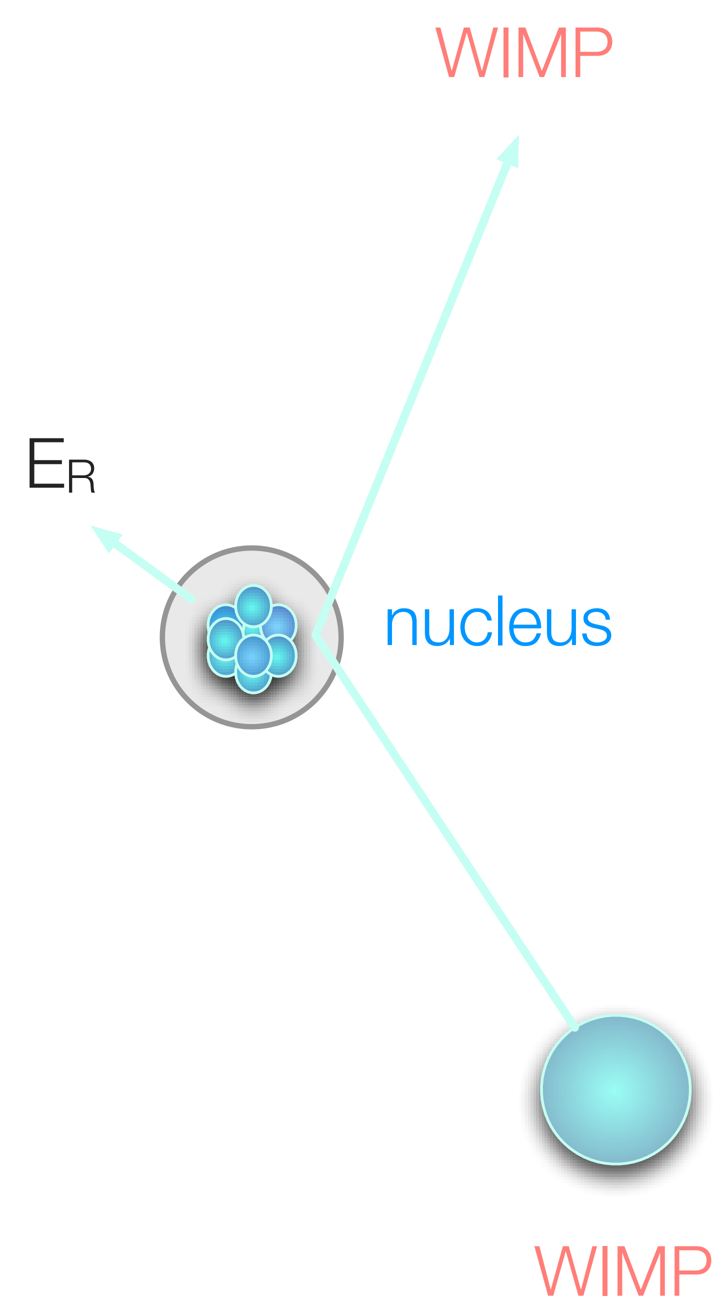

Direct detection: kinematics

- Elastic collision between WIMPs and target nuclei
- The recoil energy of the nucleus can be expressed (in the COM frame) as:

$$E_R = \frac{q^2}{2m_N} = \frac{\mu^2 v^2}{m_N}(1 - \cos\theta)$$

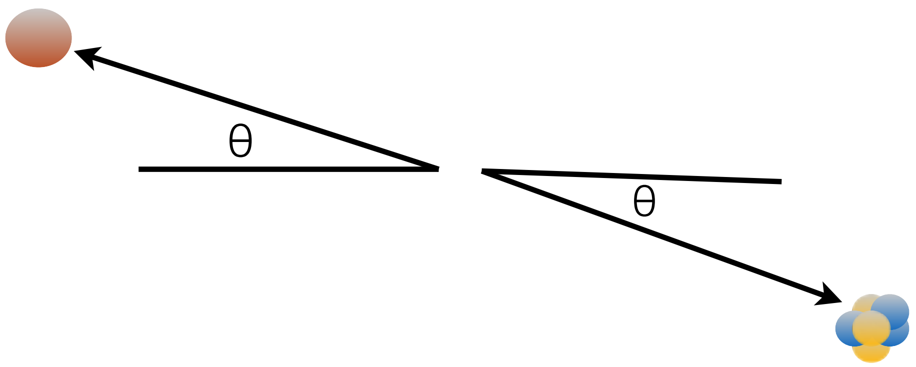

- q = momentum transfer $q^2 = 2\mu^2 v^2 (1 - \cos\theta)$
- μ = WIMP-nucleus reduced mass $\mu = \frac{m_\chi m_N}{m_\chi + m_N}$
- v = mean WIMP-velocity relative to the target (as we saw, of the order of 100 km s^{-1}, hence we are in the *extreme NR limit*)
- θ = scattering angle in the center of mass system

Direct detection: kinematics

- Hence, WIMPs with velocity v and incident kinetic energy $E_i = \frac{1}{2} m_\chi \mathrm{v}^2$ which are scattered under an angle θ in the center of mass system, will yield a recoil energy E_R in the laboratory system:

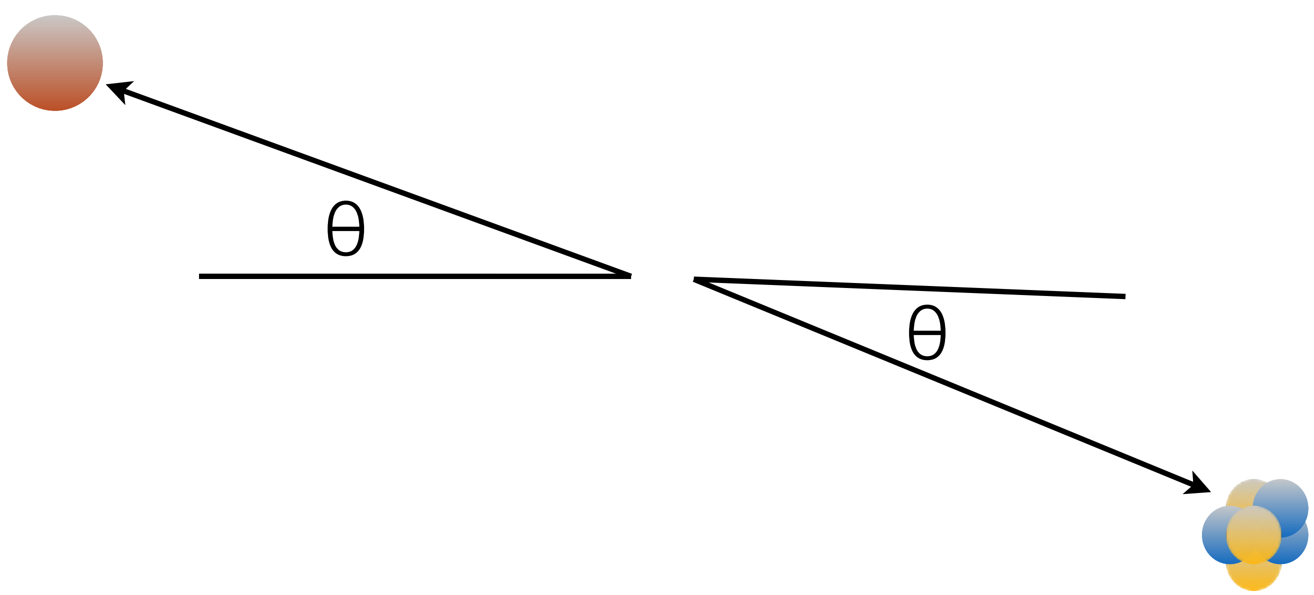

$$E_R = E_i r \frac{(1 - \cos\theta)}{2}$$

$$r = \frac{4\mu^2}{m_\chi m_N} = \frac{4 m_\chi m_N}{(m_\chi + m_N)^2}$$

WIMP nucleus reduced mass $\mu = \frac{m_\chi m_N}{m_\chi + m_N}$

A simple numerical example

- Let us assume that the WIMP mass and the nucleus mass are identical:

$$m_\chi = m_N = 100\,\mathrm{GeV} \cdot c^{-2}$$

$$\Rightarrow r = \frac{4 m_\chi m_N}{(m_\chi + m_N)^2} = 1$$

remember: r = kinematic factor

$$v \approx 220\,\mathrm{km\,s^{-1}} = 0.75 \times 10^{-3} c$$

v = mean WIMP velocity relative to target
(assumption: halo is stationary, Sun moves through halo)

$$\langle E_R \rangle = E_i = \frac{1}{2} m_\chi v^2$$

$$\langle E_R \rangle = \frac{1}{2} 100\,\frac{\mathrm{GeV}}{c^2} (0.75 \times 10^{-3})^2$$

$$\langle E_R \rangle \approx 30\,\mathrm{keV}$$

$\Rightarrow$ mean recoil energy deposited in a detector

Direct detection: momentum transfer

- With the WIMP-nucleus speed being of the order of 100 km s^{-1}, the average momentum transfer

$$\langle q \rangle \simeq \mu \langle v \rangle$$

- will be in the range between 3 MeV/c - 30 MeV/c for WIMP and nuclear masses in the range 10 GeV/c^2 - 100 GeV/c^2. Thus the elastic scattering occurs in the extreme non-relativistic limit and the scattering will be isotropic in the center of mass frame.

- The *de Broglie wavelength* corresponding to a momentum transfer of q = 10 MeV/c

$$\lambda = \frac{\hbar}{q} \simeq 20\,\mathrm{fm} > r_0 A^{1/3} = 1.25\,\mathrm{fm}\,A^{1/3}$$

- is larger than the size of most nuclei, thus the scattering amplitudes on individual nucleons will add coherently (coherence loss will be important for heavy nuclei and/or WIMPs, and WIMPs in the tail of the velocity distribution)

Expected rates in a detector: overview

$$\frac{dR}{dE_R} = N_N \frac{\rho_0}{m_W} \int_{\sqrt{(m_N E_{th})/(2\mu^2)}}^{v_{max}} dv f(v) v \frac{d\sigma}{dE_R}$$

Detector physics

N_N, E_{th}

Particle/nuclear physics

$m_W, d\sigma/dE_R$

Astrophysics

$\rho_0, f(v)$

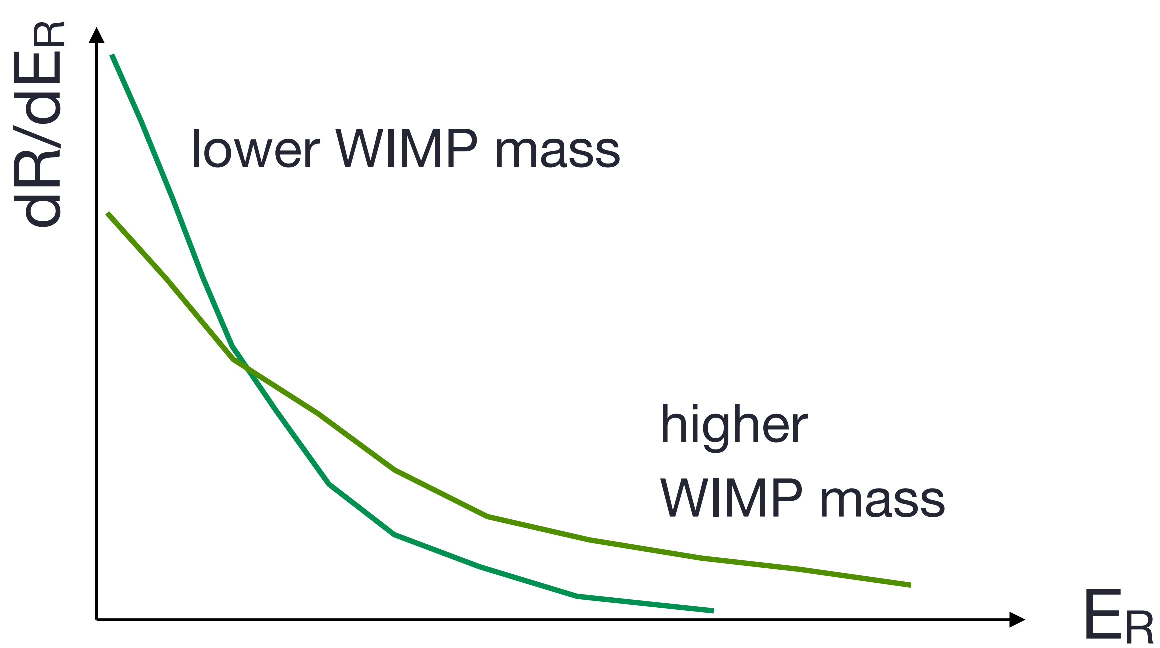

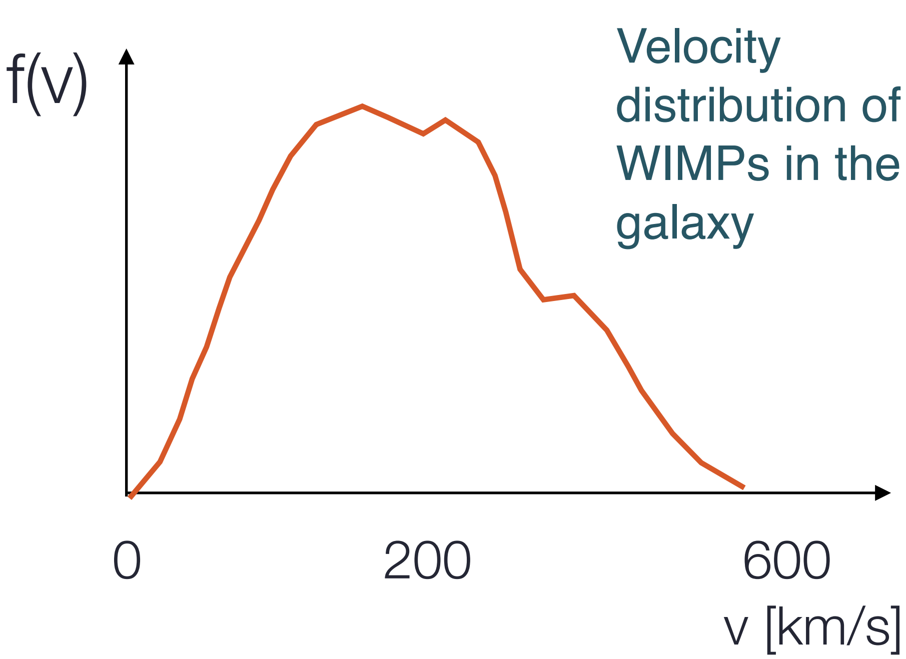

Minimum velocity

- Minimum velocity = the velocity that is required to produce a recoil energy E_R

$$v_{min} = \sqrt{\frac{2E_R}{r \cdot m_\chi}} = \sqrt{\frac{E_R m_N}{2\mu^2}} = \frac{m_\chi + m_N}{m_\chi}\sqrt{\frac{E_R}{2m_N}}$$

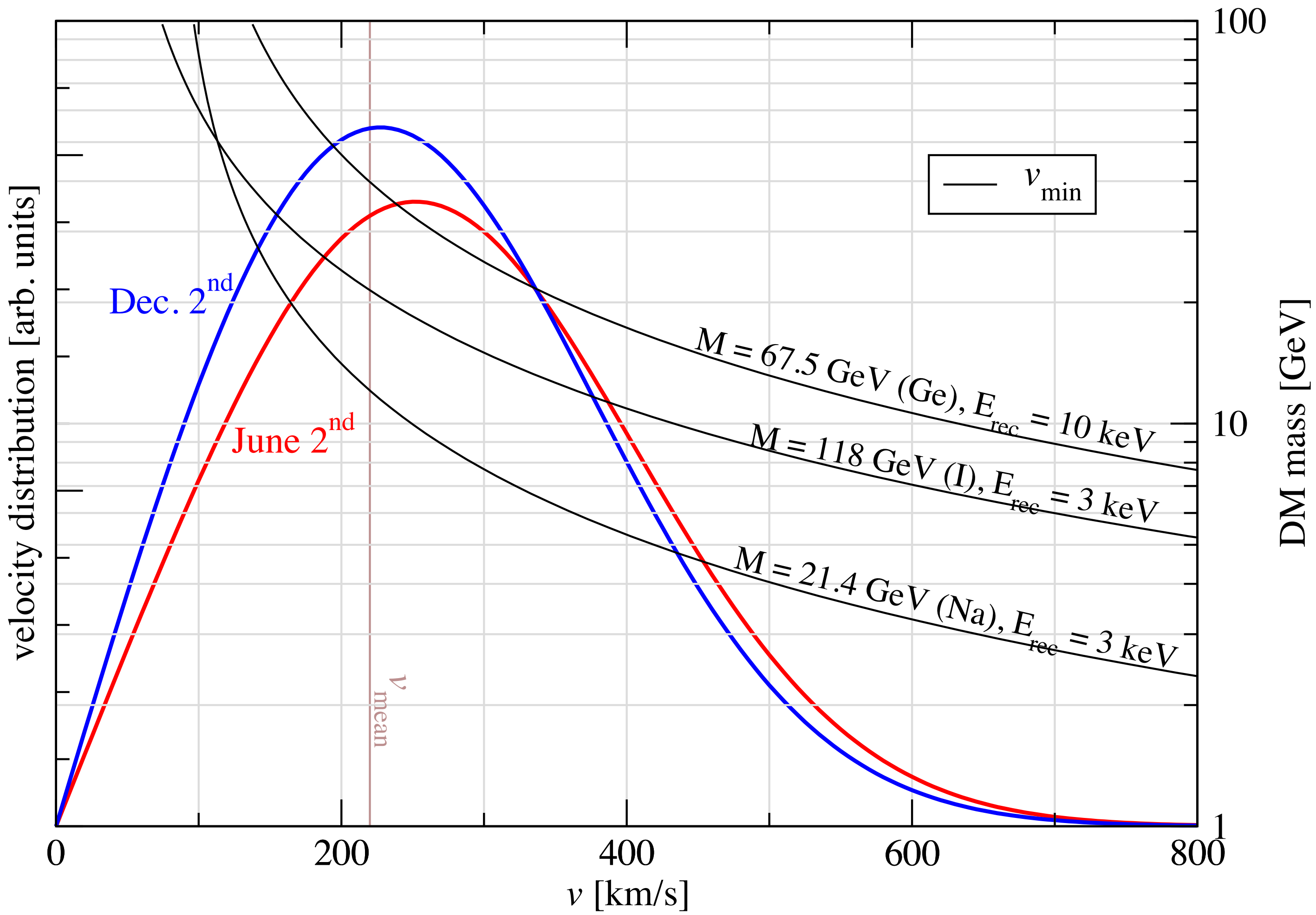

Example for v_{min} for different nuclei and E_R

WIMP-nucleus differential cross section

- **The WIMP-nucleus cross section encodes the particle physics inputs including the WIMP interaction properties**
    - It depends fundamentally on the *WIMP-quark interaction strength*, which is calculated from the microscopic description of the model, in terms of *an effective Lagrangian* describing the interaction of the WIMP candidate with quarks and gluons
    - In a next step, the *WIMP-nucleon cross section*, using hadronic matrix elements that describe the nucleon contents in the quarks, is calculated
    - In a third step, using nuclear wave functions, the spin and the scalar components of nucleons are added to obtain *the matrix element of WIMP-nucleus cross section* as a function of momentum transfer. This step introduces a form factor suppression which reduces the cross section for heavy WIMPs and/or nuclei (analogous to low-energy electromagnetic scattering of electrons from nuclei)

- **Important simplification: the elastic scattering takes place in the extreme NR limit, 2 cases are mostly considered:**
    - spin-spin interactions (coupling to the nuclear spin)
    - scalar interactions (coupling to the mass of the nucleus)

WIMP-nucleus differential cross section

- **The WIMP-nucleus cross section encodes the particle physics inputs including the WIMP interaction properties**
  - ◉ It depends fundamentally on the WIMP-quark interaction strength, which is calculated from the microscopic description of the model, in terms of an effective Lagrangian describing the interaction of the WIMP candidate with quarks and gluons
  - ◉ In a next step, the WIMP-nucleon cross section, using hadronic matrix elements that describe the nucleon contents in the quarks, is calculated
  - ◉ In a third step, using nuclear wave functions, the spin and the scalar components of nucleons are added to obtain the matrix element of WIMP-nucleus cross section as a function of momentum transfer. This step introduces a form factor suppression which reduces the cross section for heavy WIMPs and/or nuclei (analogous to low-energy electromagnetic scattering of electrons from nuclei)
- In recent years: efforts to treat WIMP interactions more generally, using the tools of EFT
  - ◉ one writes down all WIMP-nucleon operators consistent with general symmetry arguments
  - ◉ then the interactions are imbedded in the nucleus → nuclear operators → response functions that describe the WIMP-nucleus elastic scattering

see, e.g, Fitzpatrick et al., JCAP 1302 (2013) “The effective field theory of dark matter direct detection”
M. Hoferichter et al., PRD 94 (2016) 6 “Analysis strategies for general spin-independent WIMP-nucleus scattering”

Scattering cross sections and effective operators

- Use effective operators to describe WIMP-quark interactions

- Example: vector mediator

contact interaction scale

$$\mathcal{L}_\chi^{\text{eff}} = \frac{1}{\Lambda^2}\bar{\chi}\gamma_\mu\chi\bar{q}\gamma^\mu q \qquad \Lambda = \frac{M}{\sqrt{g_q g_\chi}} \Rightarrow \sigma_{\text{tot}} \propto \Lambda^{-4}$$

- The effective operator arises from “integrating out” the mediator with mass M and couplings g_q and g_χ to the quark and the WIMP

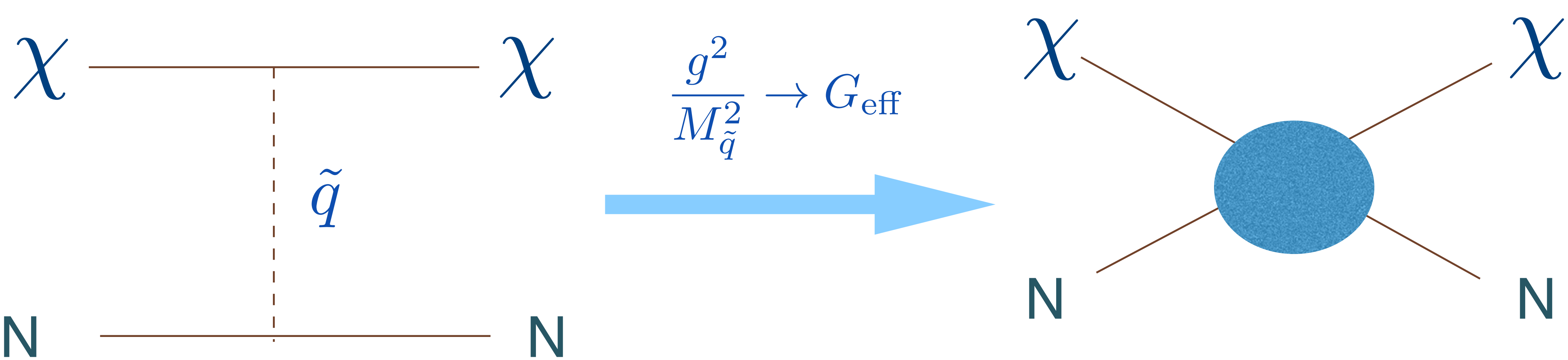

Scattering cross sections and effective operators

- Use effective operators to describe WIMP-quark interactions (also called NREFT approach):
  - after adding a dark matter particle to the SM, choosing a spin and EW representation, add interactions with quarks and gluons, consistent with the exact symmetries of the SM: write down all possible operators
  - certain operators will contribute to SI or to SD WIMP scattering at zero velocity
  - many operators have very weak direct detection bounds due to the velocity suppression of the scattering

Name	Operator	Coefficient
D1	$\bar{\chi}\chi\bar{q}q$	m_q/M_*^3
D2	$\bar{\chi}\gamma^5\chi\bar{q}q$	im_q/M_*^3
D3	$\bar{\chi}\chi\bar{q}\gamma^5 q$	im_q/M_*^3
D4	$\bar{\chi}\gamma^5\chi\bar{q}\gamma^5 q$	m_q/M_*^3
D5	$\bar{\chi}\gamma^\mu\chi\bar{q}\gamma_\mu q$	$1/M_*^2$
D6	$\bar{\chi}\gamma^\mu\gamma^5\chi\bar{q}\gamma_\mu q$	$1/M_*^2$
D7	$\bar{\chi}\gamma^\mu\chi\bar{q}\gamma_\mu\gamma^5 q$	$1/M_*^2$
D8	$\bar{\chi}\gamma^\mu\gamma^5\chi\bar{q}\gamma_\mu\gamma^5 q$	$1/M_*^2$
D9	$\bar{\chi}\sigma^{\mu\nu}\chi\bar{q}\sigma_{\mu\nu}q$	$1/M_*^2$
D10	$\bar{\chi}\sigma_{\mu\nu}\gamma^5\chi\bar{q}\sigma_{\alpha\beta}q$	i/M_*^2
D11	$\bar{\chi}\chi G_{\mu\nu}G^{\mu\nu}$	$\alpha_s/4M_*^3$
D12	$\bar{\chi}\gamma^5\chi G_{\mu\nu}G^{\mu\nu}$	$i\alpha_s/4M_*^3$
D13	$\bar{\chi}\chi G_{\mu\nu}\tilde{G}^{\mu\nu}$	$i\alpha_s/4M_*^3$
D14	$\bar{\chi}\gamma^5\chi G_{\mu\nu}\tilde{G}^{\mu\nu}$	$\alpha_s/4M_*^3$

Goodman, Ibe, Rajaraman, Shepherd, Tait, Yu 2010

More recently: chiral effective field theory ChEFT (in NREFT, the operators are not independent of one another due to QCD effects), see, e.g. M. Hoferichter et al., PRD 99, 2019

Spin independent cross section

- The differential cross section can be written as:

$$\frac{d\sigma(q)}{dq^2} = \frac{\sigma_0 F^2(q)}{4\mu^2 \mathrm{v}^2}$$

→ relative velocity in center-of-mass frame

- where σ_0 = total cross section for F(q) = 1.

- From Fermi's Golden Rule it follows:

$$\frac{d\sigma(q)}{dq^2} = \frac{1}{\pi \mathrm{v}^2}|M|^2 = \frac{1}{\pi \mathrm{v}^2} f_n^2 A^2 F^2(q)$$

- One can then identify the total cross section σ_0 for F(q)=1 as:

$$\sigma_0 = \frac{4\mu^2}{\pi} f_n^2 A^2 = \underbrace{\frac{4}{\pi} m_n^2 f_n^2}_{\sigma_n} \frac{\mu^2}{m_n^2} A^2$$

cross section for scattering off nucleus → σ_0

cross section for scattering on nucleons: σ_n → dependence on particle physics model for WIMP

Spin independent cross section

- Putting now everything together:

$$\frac{d\sigma(q)}{dq^2} = \frac{1}{4m_n^2 v^2}\sigma_n A^2 F^2(q)$$

differential cross section

$$\frac{dR}{dE_R} = \frac{R_0}{E_0 r} e^{-\frac{E_R}{E_0 r}} F^2(q)$$

differential recoil energy spectrum

particle physics

dark matter halo

$$R_0 = \frac{2}{\sqrt{\pi}} \frac{N_A}{A} \frac{\rho_\chi}{m_\chi} \sigma_0 \, v_0$$

$$\sigma_0 = \sigma_n \frac{A^2}{m_n^2} \left(\frac{m_\chi m_N}{m_\chi + m_N} \right)^2$$

detector

Spin independent cross section

- **As we saw, interactions leading to WIMP-nucleus scattering are parameterised:**
  - **scalar interactions** (coupling to WIMP mass, from scalar, vector, tensor part of L)

$$\sigma_{SI} \sim \frac{\mu^2}{m_\chi^2}[Zf_p + (A-Z)f_n]^2$$

f_p, f_n: scalar 4-fermion couplings to p and n

⇒ nuclei with large A favourable (but see nuclear form factor corrections)

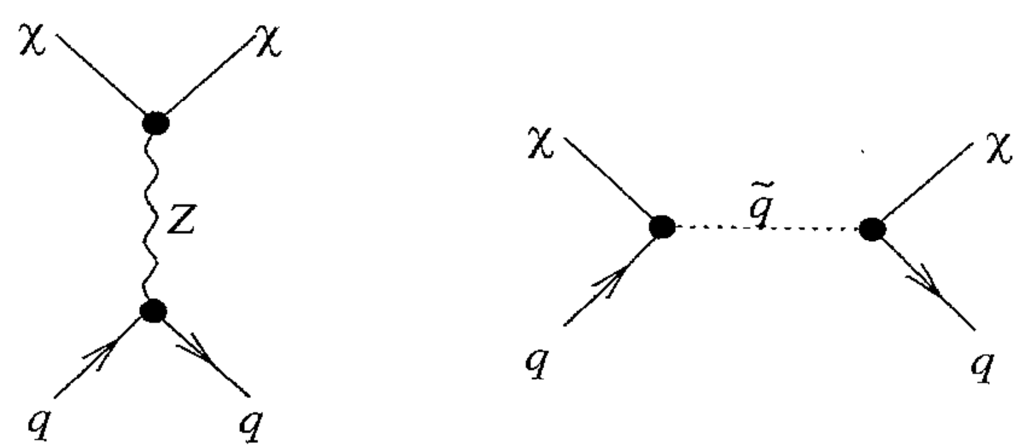

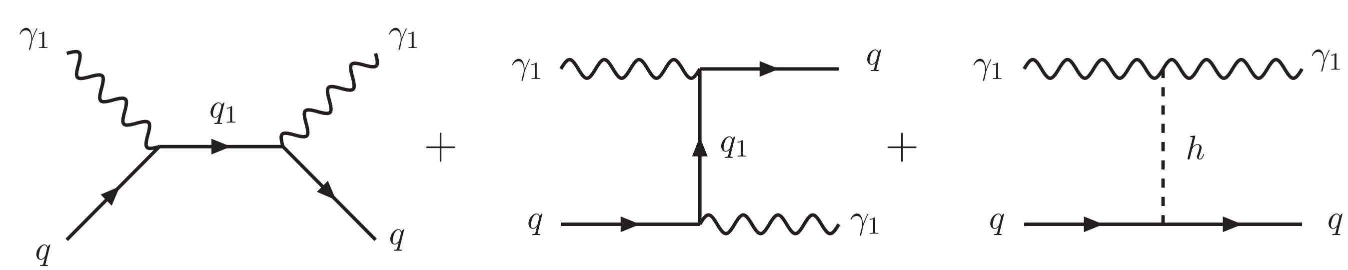

Spin dependent cross section

- **As we saw, interactions leading to WIMP-nucleus scattering are parameterised:**
  - **spin-spin interactions** (coupling to the nuclear spin J_N, from axial-vector part of L)

$$\sigma_{SD} \sim \mu^2 \frac{J_N + 1}{J_N} (a_p \langle S_p \rangle + a_n \langle S_n \rangle)^2$$

a_p, a_n: effective couplings to p and n; $\langle S_p \rangle$ and $\langle S_n \rangle$ expectation values of the p and n spins within the nucleus

⇒ nuclei with non-zero angular momentum (corrections due to spin structure functions)

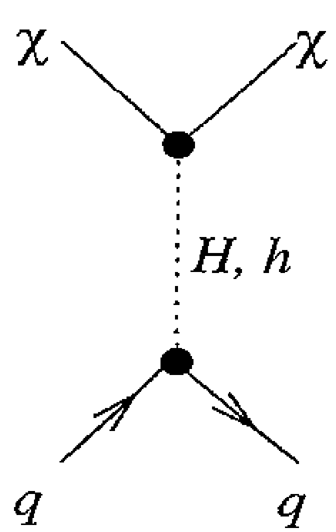

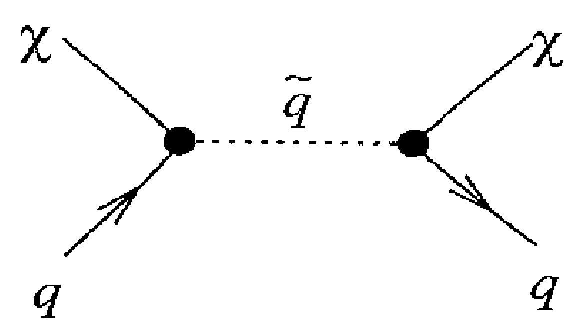

Cross sections on nucleons: examples

◉ Predictions from supersymmetry for the neutralino [10^{-8} pb = 10^{-44} cm^2]:

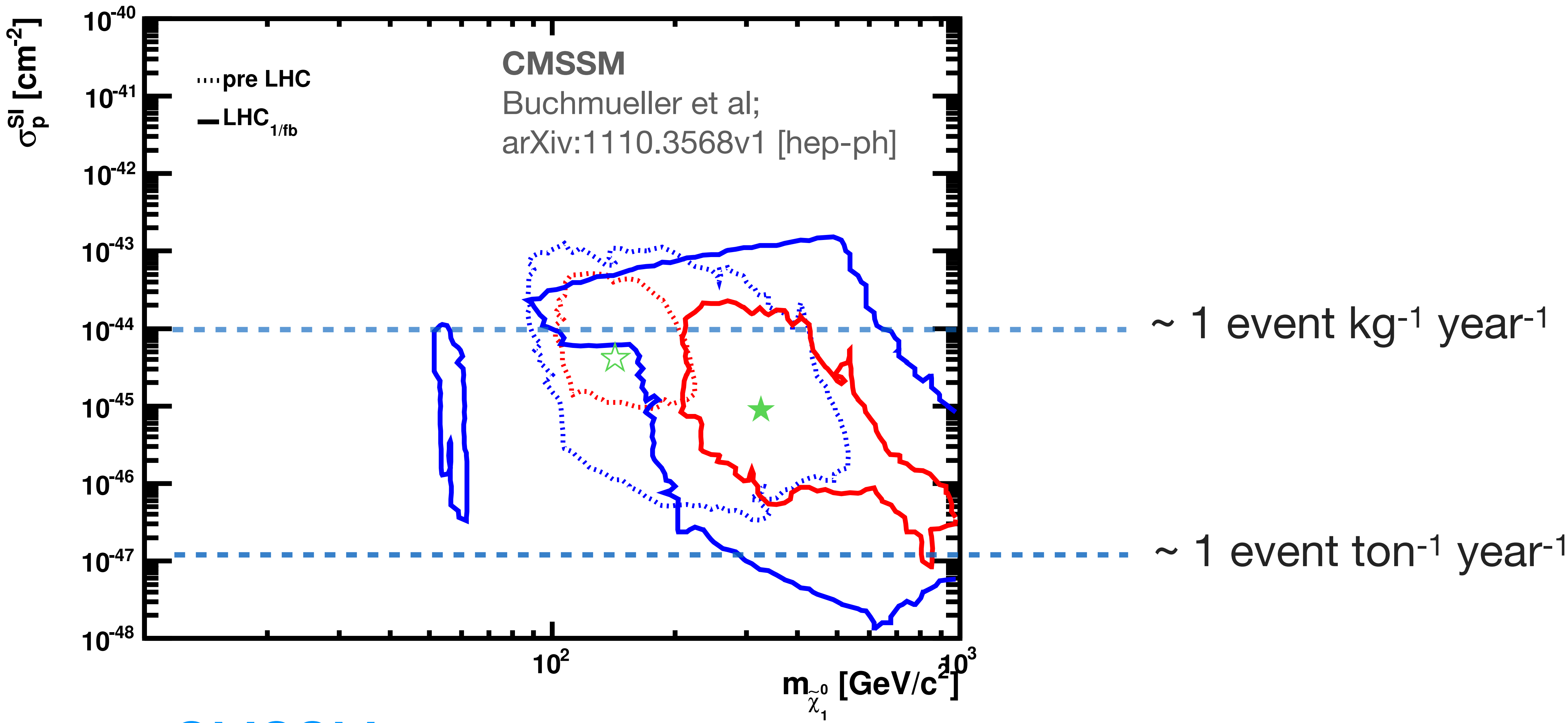

CMSSM

Cross sections on nucleons: examples

◉ Predictions from supersymmetry for the neutralino [10^{-8} pb = 10^{-44} cm^2]:

CMSSM

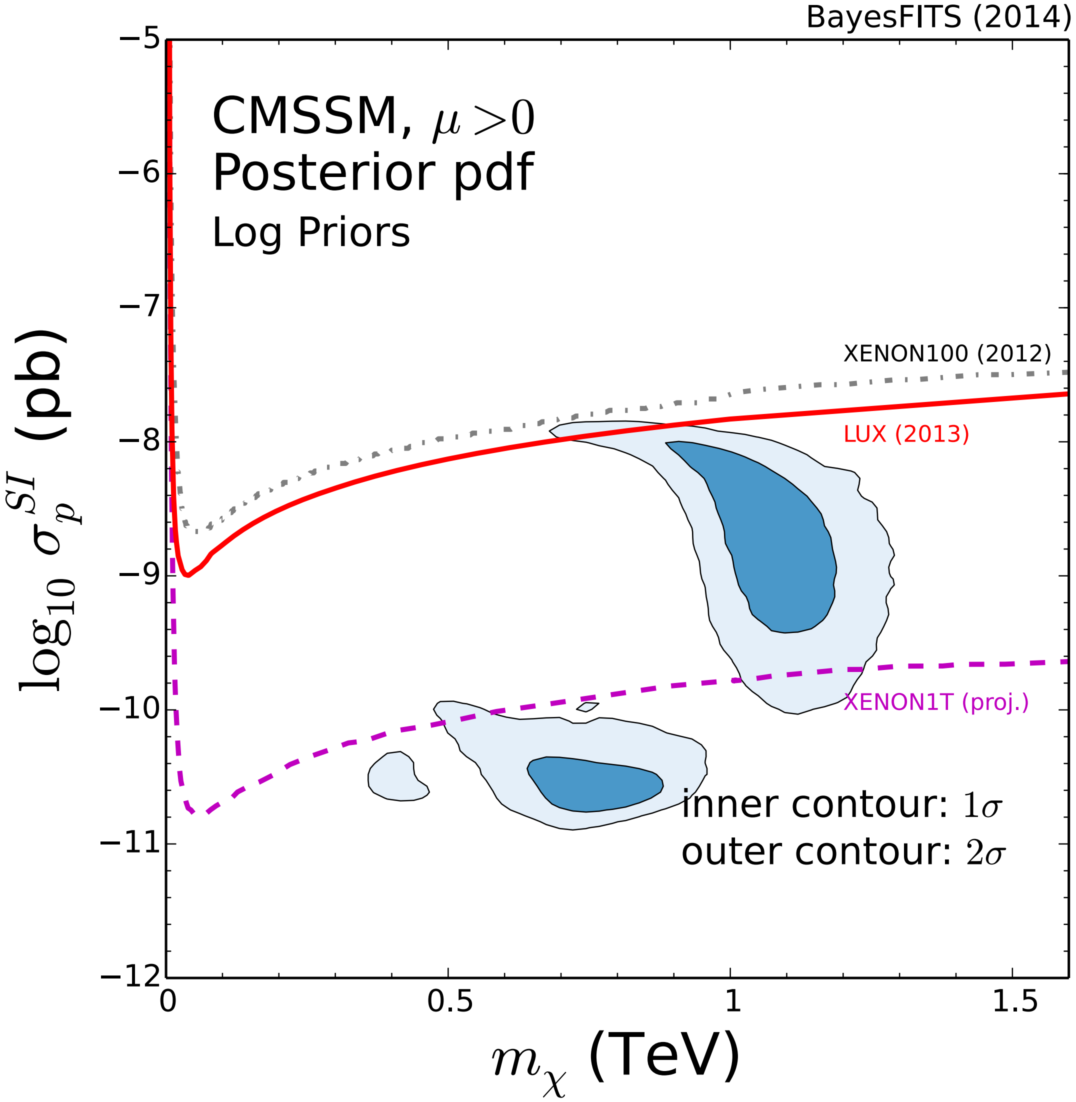

L. Rozkowski, Stockholm 2015

pMSSM

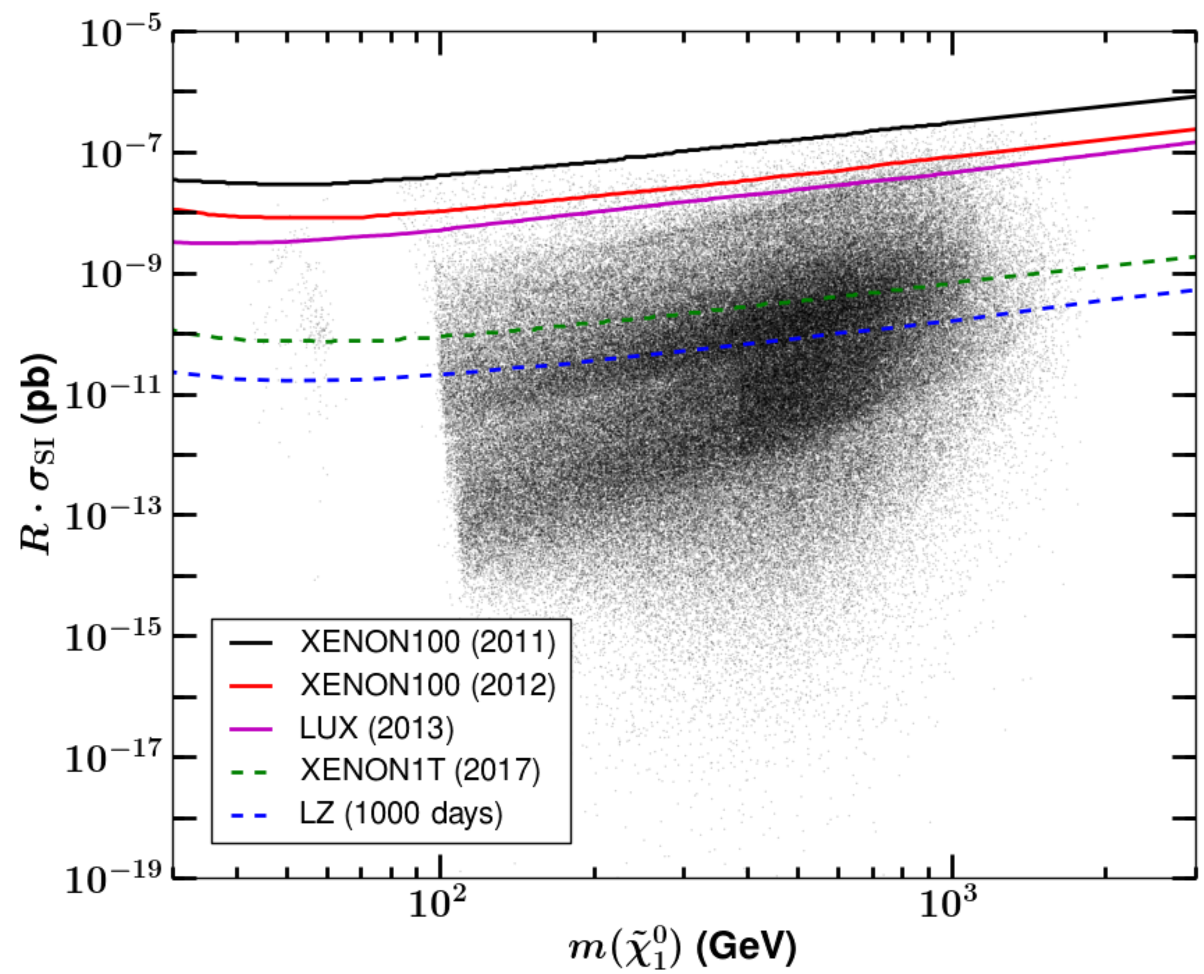

M. Cahill-Rowley, Phys.Rev. D91 (2015) 055011

Cross sections on nucleons: examples

- SI scattering cross sections for various "visible sector" models

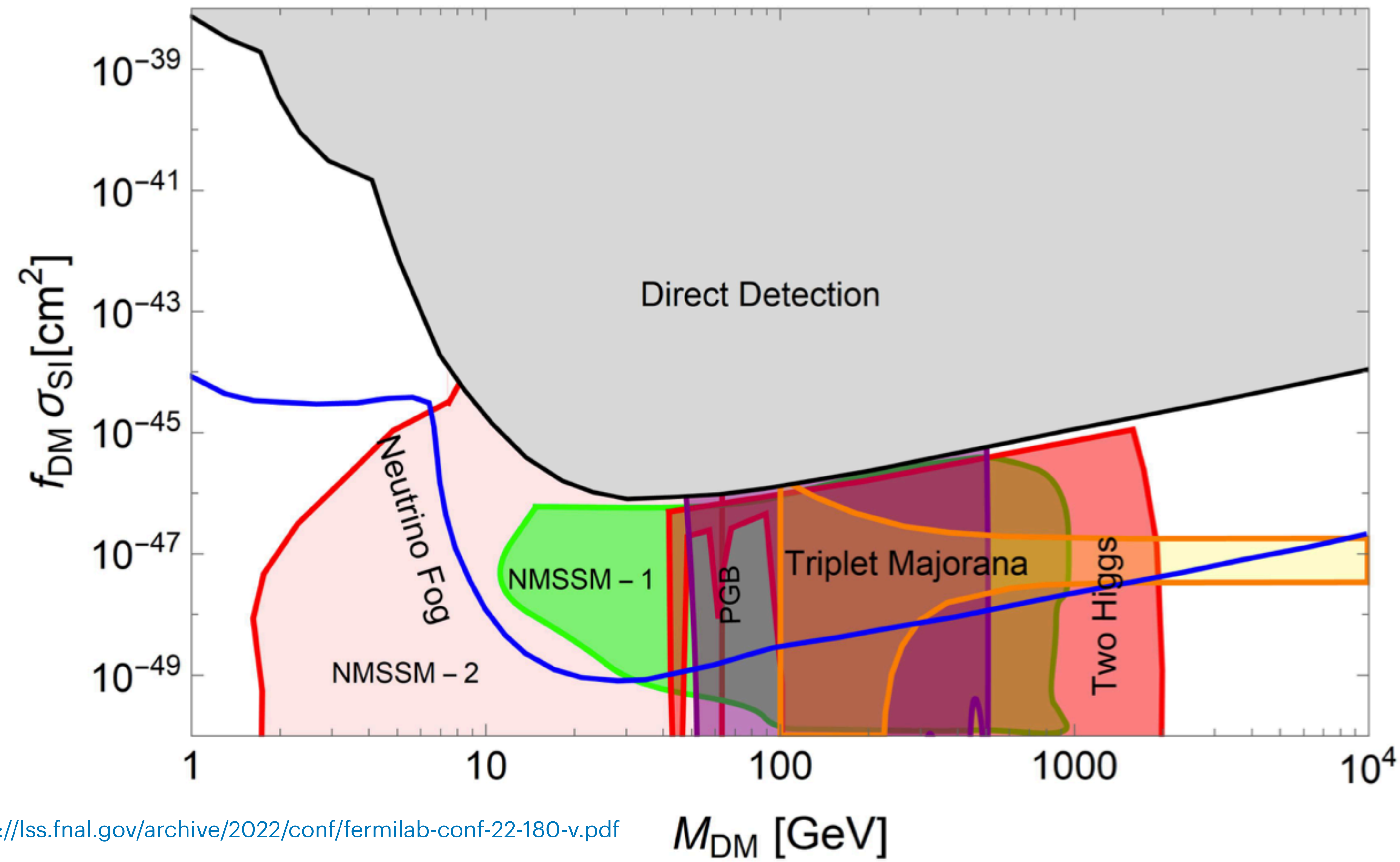

https://lss.fnal.gov/archive/2022/conf/fermilab-conf-22-180-v.pdf

Nuclear form factors: SI couplings

- Scattering amplitude: Born approximation $\vec{q} = \hbar\,(\vec{k}' - \vec{k})$
- Spin-independent scattering is coherent $\lambda = \hbar/q \sim$ few fm

$q = \sqrt{2 m_N E_R}$

$$M(\vec{q}) = f_n\, A \underbrace{\int d^3x\, \rho(\vec{x})\, e^{i\,\vec{q}\cdot\vec{x}}}_{F(\vec{q})} \quad \Rightarrow \quad \sigma \propto |M|^2 \propto A^2$$

mass number

fundamental couplings to nucleons

Fourier-transform of the density of scattering centres

$$F(qr_n) = \underbrace{\frac{3[\sin(qr_n) - qr_n\cos(qr_n)]}{(qr_n)^3}}_{j_1(qr_n)}\, e^{-(qs)^2/2}$$

"Helm" form factor

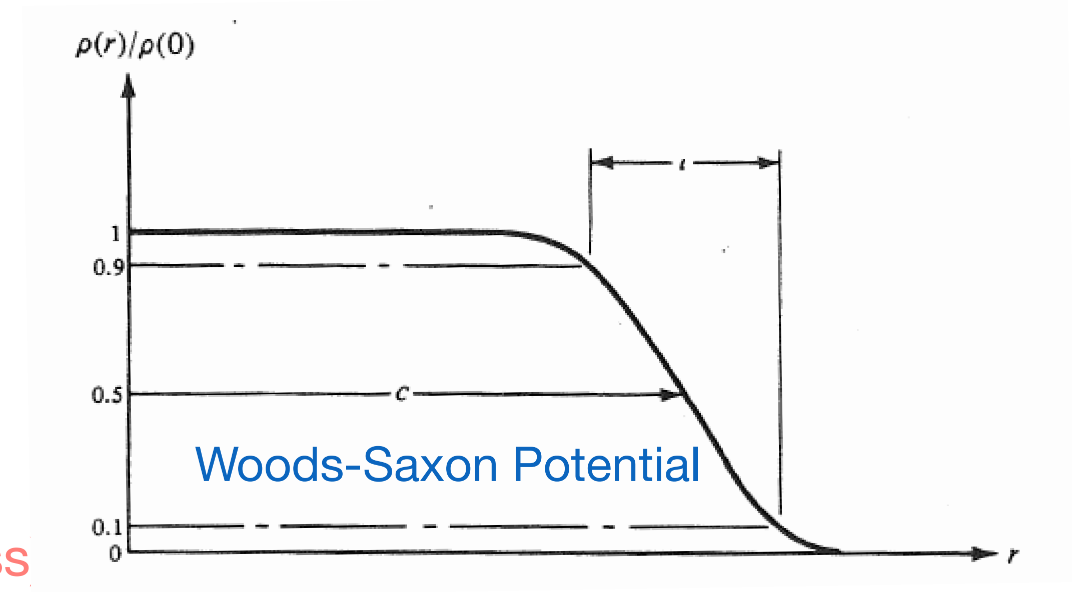

- with r_n = nuclear radius, $r_n \approx 1.2\, A^{1/3}$ fm, s = 1fm (skin thickness

Nuclear form factors: SI couplings

- Important for heavy WIMPs and/or nuclei and for WIMPs in the tail of f(v)
- Helm form factor: Fourier-transform of the density of scattering centres

$$\frac{d\sigma_{SI}}{dq^2} = \sigma_{0,SI} \times S_s(q)$$

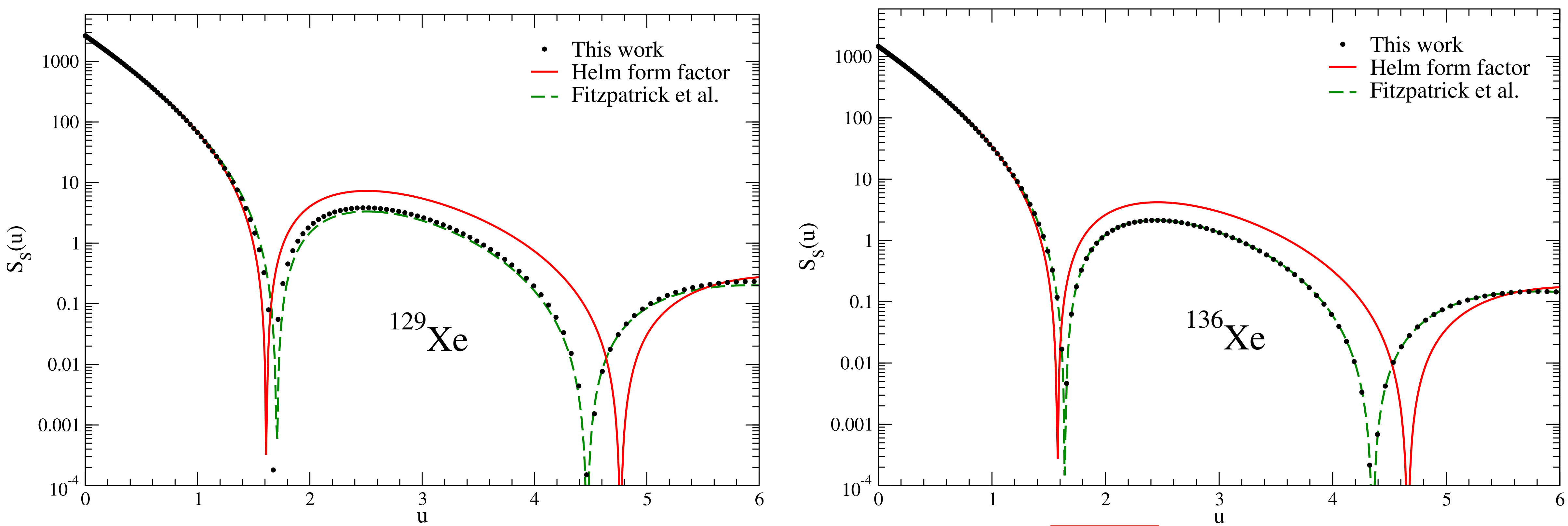

$$u = q^2 b^2 / 2 \qquad b = \sqrt{\bar{h}/m\omega}$$

b = harmonic oscillator size parameter

L. Vietze et al., Phys.Rev. D91 (2015) 4, 043520

Nuclear form factors: SD couplings

- For spin-dependent couplings the scattering amplitude is dominated by the unpaired nucleon: the coupling is to the total nuclear spin J (paired nucleons ↑↓ tend to cancel):

$$\frac{d\sigma(q)}{dq^2} = \frac{8}{\pi v^2}\Lambda^2 G_F^2 J(J+1)F^2(q)$$

- with: G_F = Fermi constant, J = nuclear spin, $F^2(q)$ = form factor for spin dependent interactions

- and $$\Lambda = \frac{1}{J}\left[a_p\langle S_p\rangle + a_n\langle S_n\rangle\right]$$

- a_p, a_n: effective coupling of the WIMPs to protons and neutrons

- and the expectation values of the proton and neutron spins in the nucleus

$$\langle S_{p,n}\rangle = \langle N|S_{p,n}|N\rangle$$

measure the amount of spin carried by the p- and n-groups inside the nucleus

Nuclear form factors: SD couplings

- Form factor example: simplified, based on model with valence nucleons in a thin shell:

$$F(qr_n) = j_0(qr_n) = \frac{\sin(qr_n)}{qr_n}$$

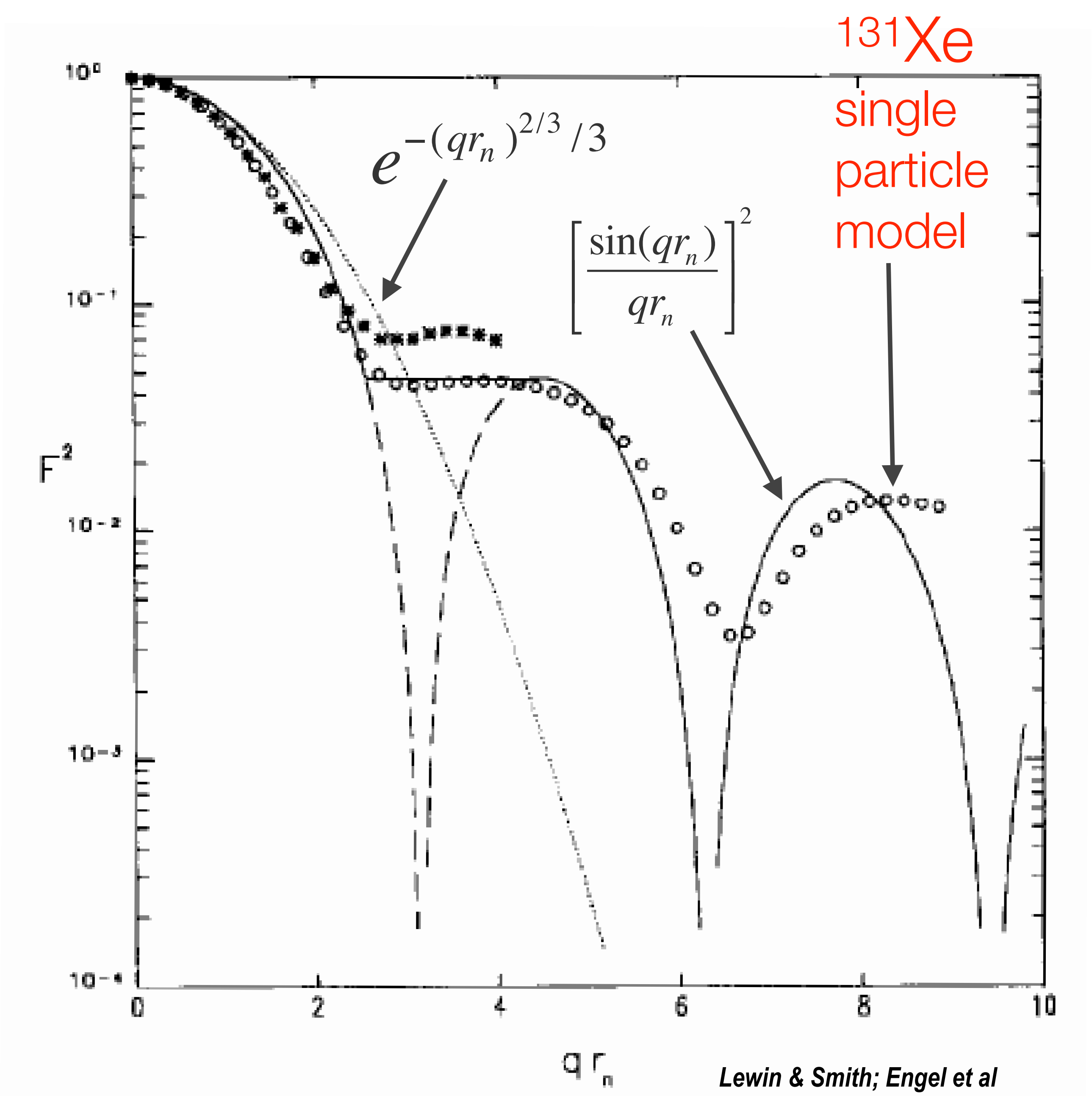

- Better: detailed calculations based on realistic nuclear models
  -for instance, the conventional nuclear shell model using reasonable nuclear Hamiltonians
  - cross check by agreement of predicted versus measured magnetic moment of the nucleus (since the matrix element for χN scattering is similar to the magnetic moment operator)

Nuclear form factors: SD couplings

- WIMP-nucleus response based on detailed nuclear structure calculations

$$\frac{d\sigma_{SD}}{dq^2} = \sigma_{0,SD} \times S_A(q)$$

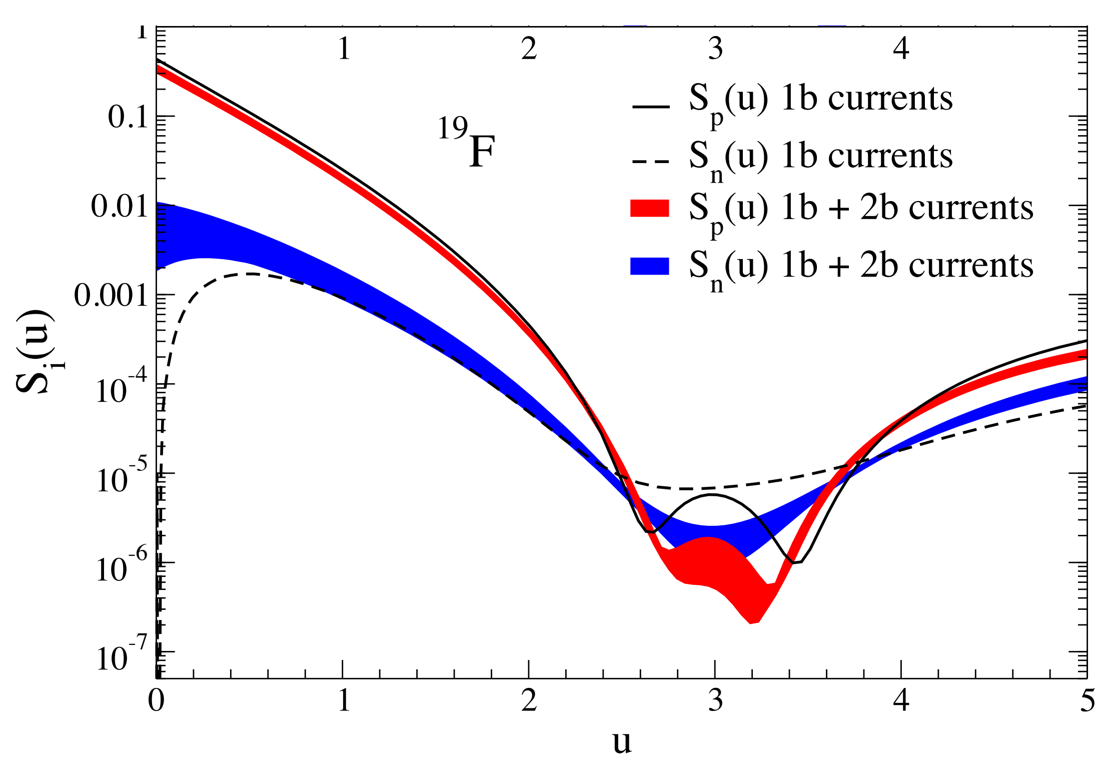

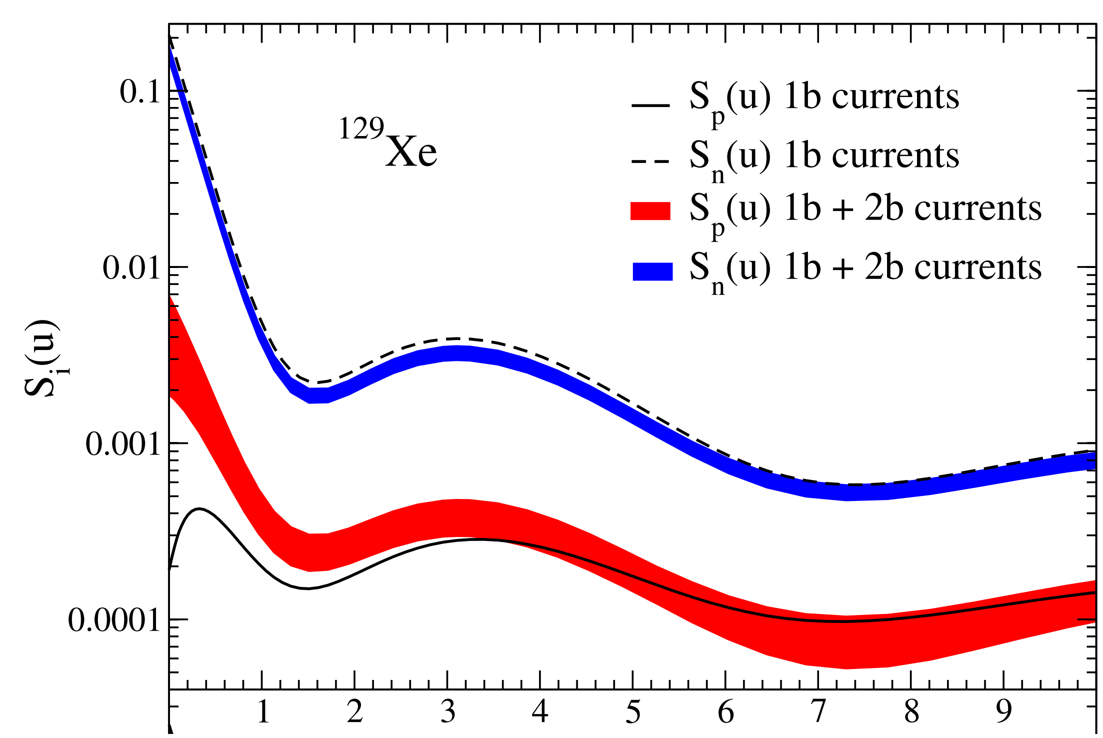

$u = q^2 b^2 / 2$ $\quad b = \sqrt{\bar{h}/m\omega}$ b = harmonic oscillator size parameter

P. Klos et al., PRD 88, 2013

Nuclear form factors: SD couplings

- WIMP-nucleus response based on detailed nuclear structure calculations

$$\frac{d\sigma_{SD}}{dq^2} = \sigma_{0,SD} \times S_A(q)$$

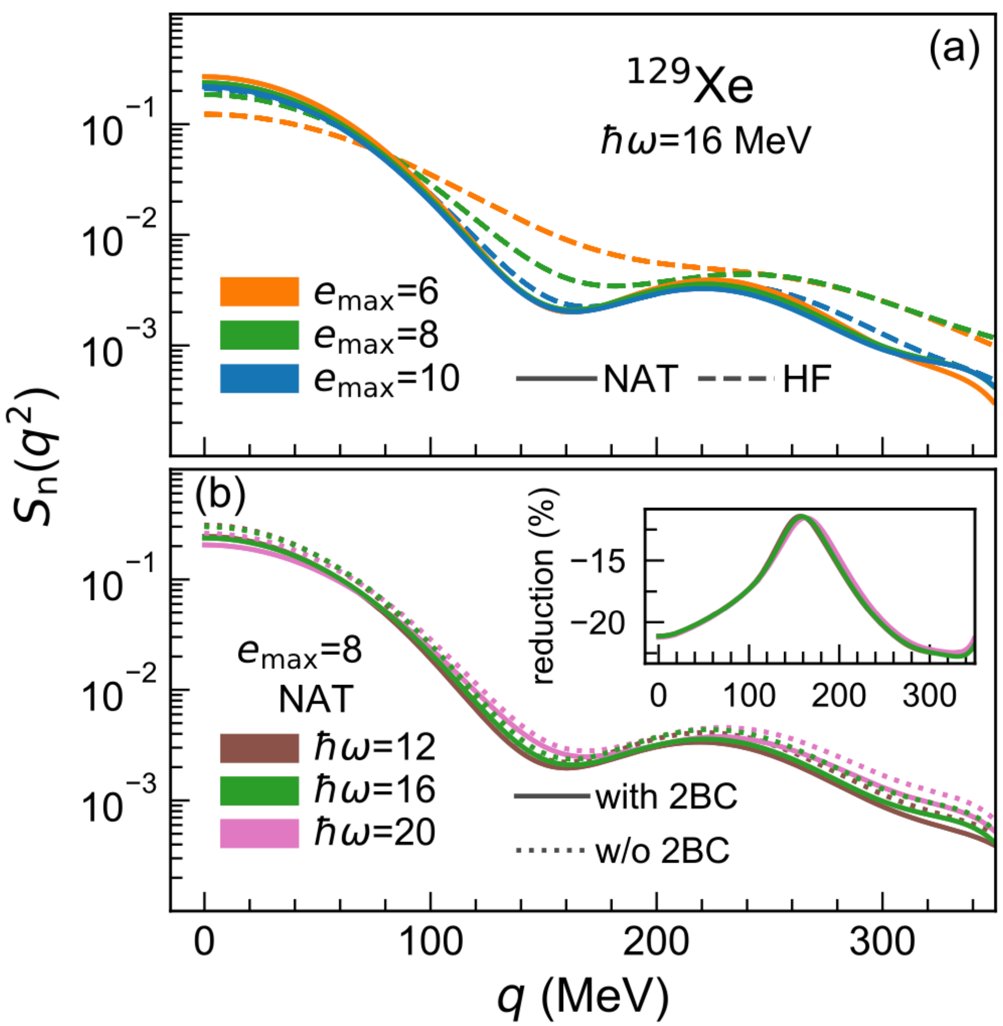

B.S. Hu et al, PRL 128, 2022

Putting it all together: expected differential rates

$$R \sim 0.13 \; \frac{\text{events}}{\text{kg year}} \left[\frac{A}{100} \times \frac{\sigma_{WN}}{10^{-38}\,\text{cm}^2} \times \frac{\langle v \rangle}{220\,\text{km}\,\text{s}^{-1}} \times \frac{\rho_0}{0.3\,\text{GeV}\text{cm}^{-3}} \right]$$

$$v_{min} = \sqrt{\frac{m_N E_{th}}{2\mu^2}}$$

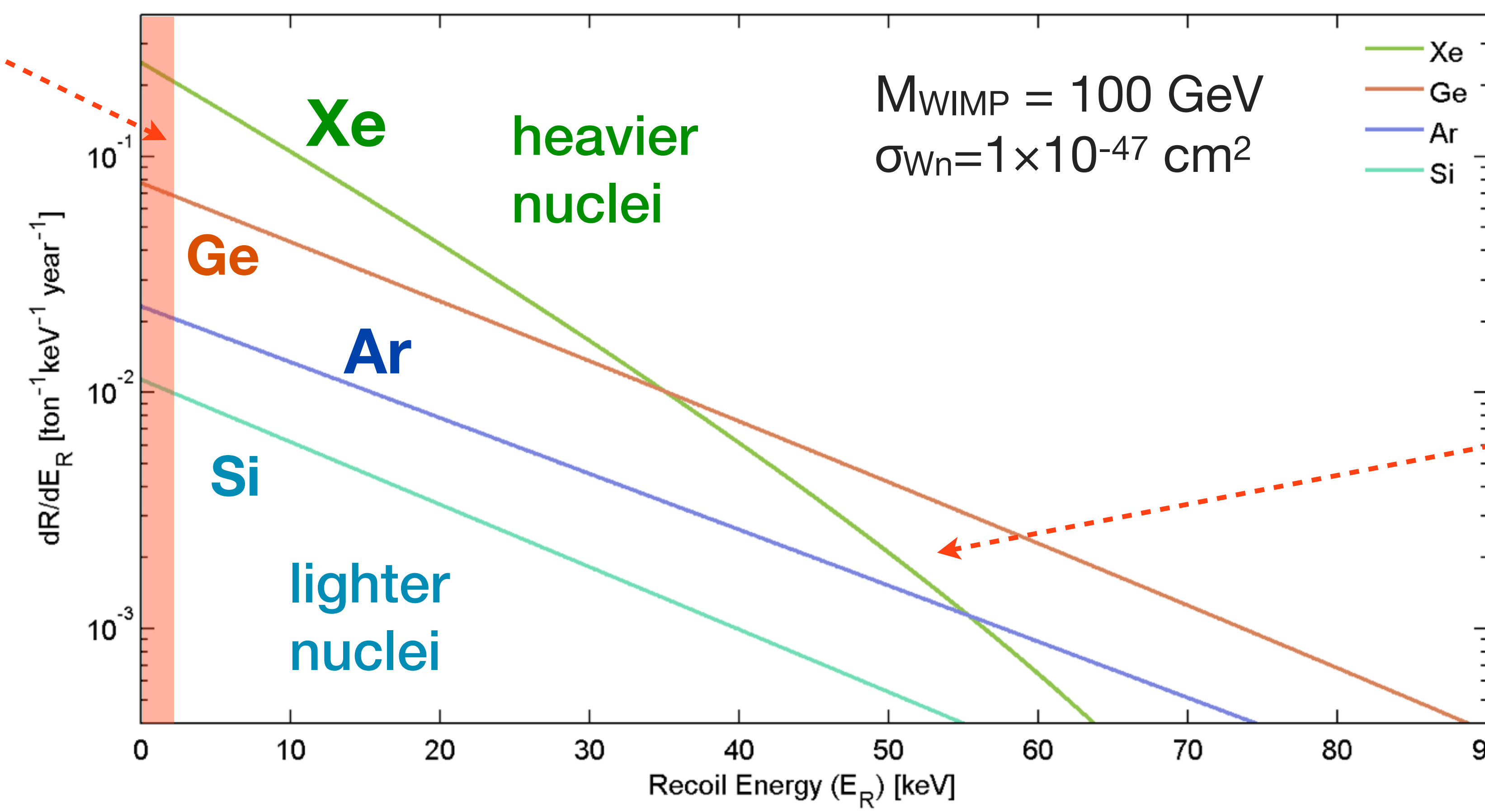

F²(E_R)

Dependance on the WIMP mass

- Recoil spectrum gets shifted to low energies for low WIMP masses
- One needs a light target and/or a low energy threshold to see light WIMPs

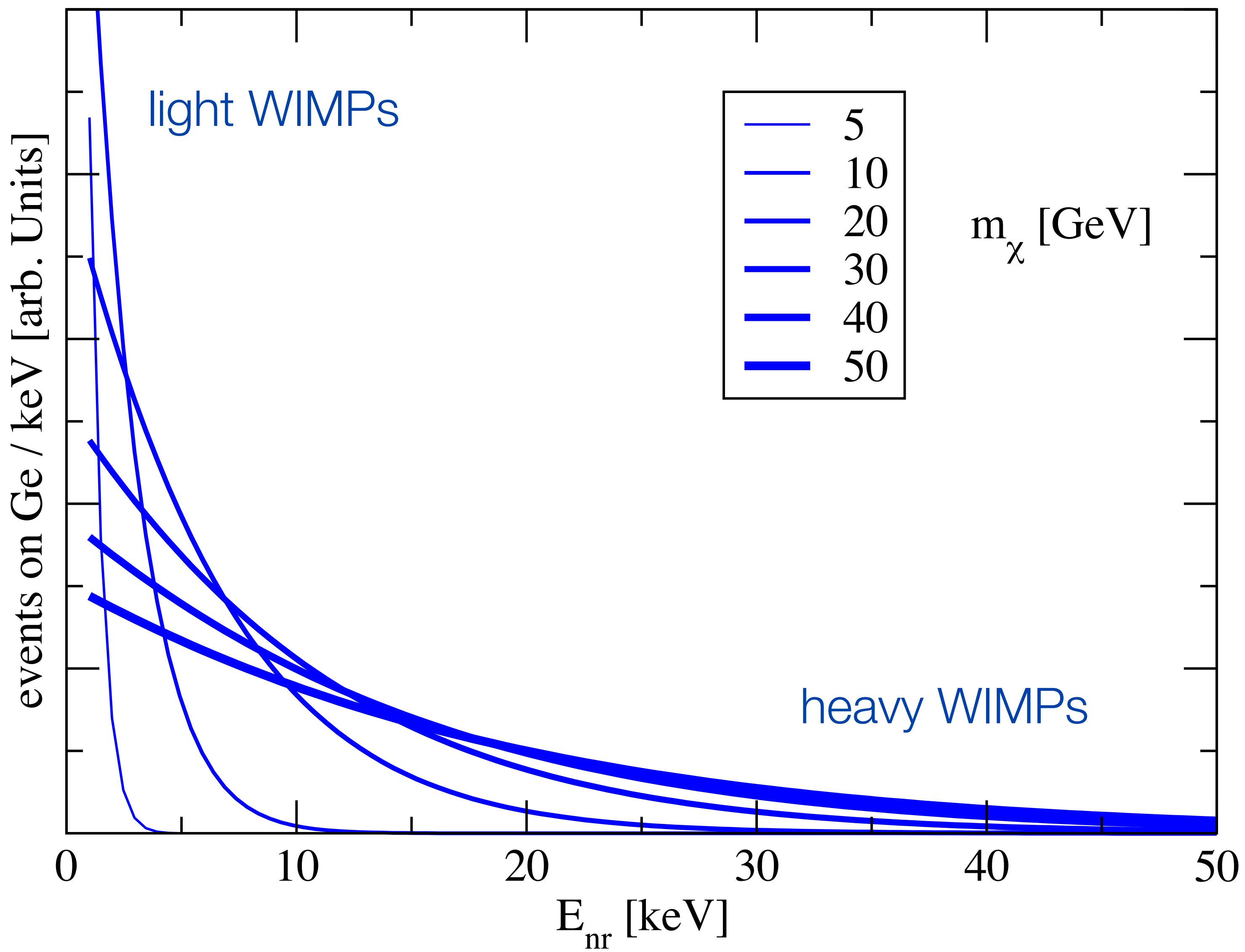

Summary on expected rates in a detector

- One has to take into account following facts:
  - the WIMPs have a certain velocity distribution f(v)
  - the detector is on Earth, which moves around the Sun, which moves around the Galactic Center
  - the cross section depends on whether the interaction is spin-independent (SI), or spin-dependent (SD)
  - the WIMPs scatter on nuclei, which have a finite size; we had to consider form-factor corrections < 1 (different for SI and SD interactions)
  - the nuclear recoil energy is not necessarily the *observed* energy, since in general the detection efficiency is < 1
  - detectors have a certain energy resolution and energy threshold

observed diff. rate →

$$\Rightarrow \frac{dR}{dE_R} = R_0 S(E_R) F^2(E_R) I$$

spectral function (masses and kinematics) → $S(E_R)$

form factor correction → $F^2(E_R)$

type of interaction → I

Cross section versus DM particle mass: limit plot

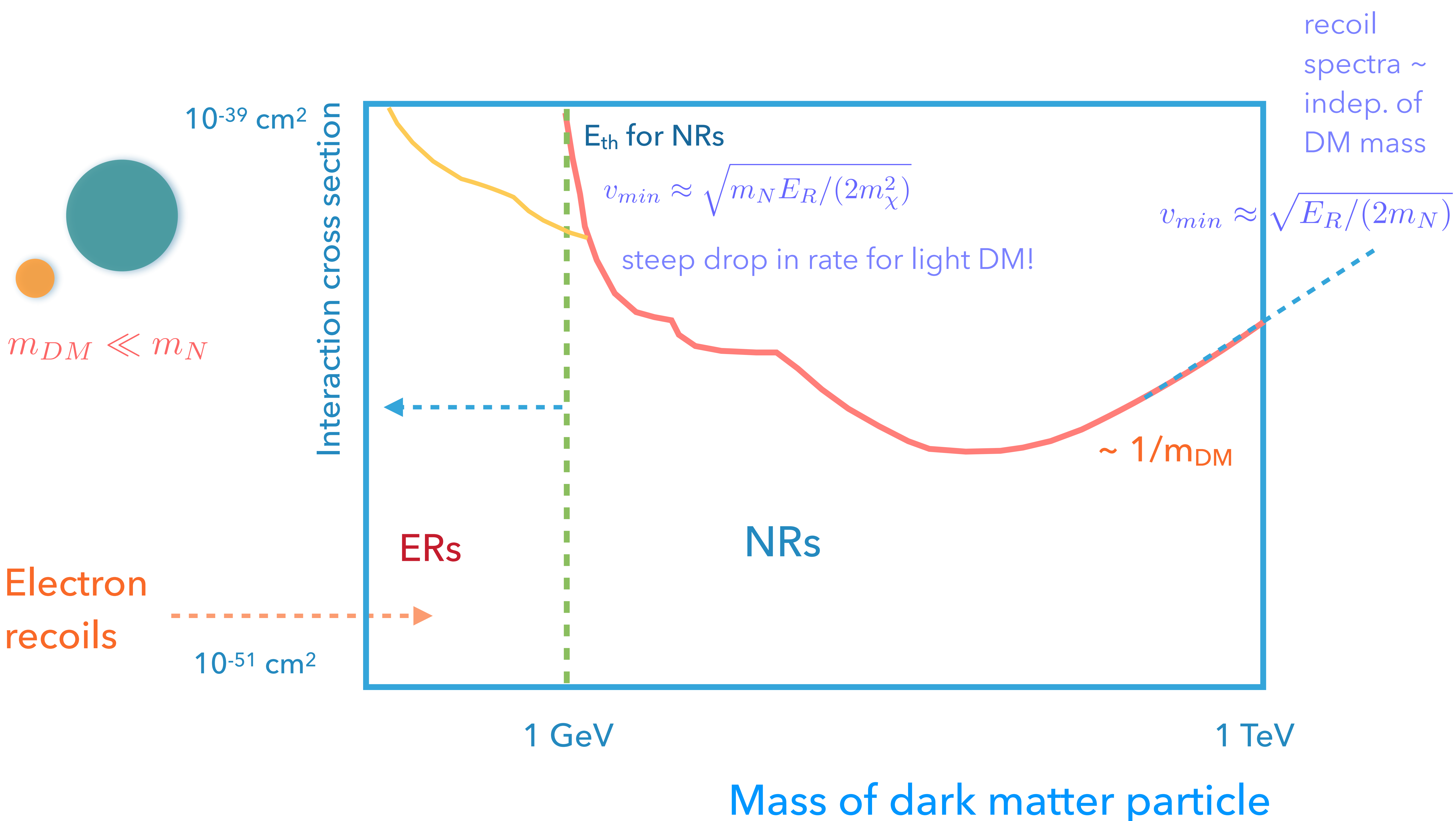

Cross section versus DM particle mass: evidence

- In case of a detection: one aims to reconstruct the DM mass and cross section (here shown for various DM masses, 25, 50, 250 GeV/c^2, and one cross sections

fixed galactic model

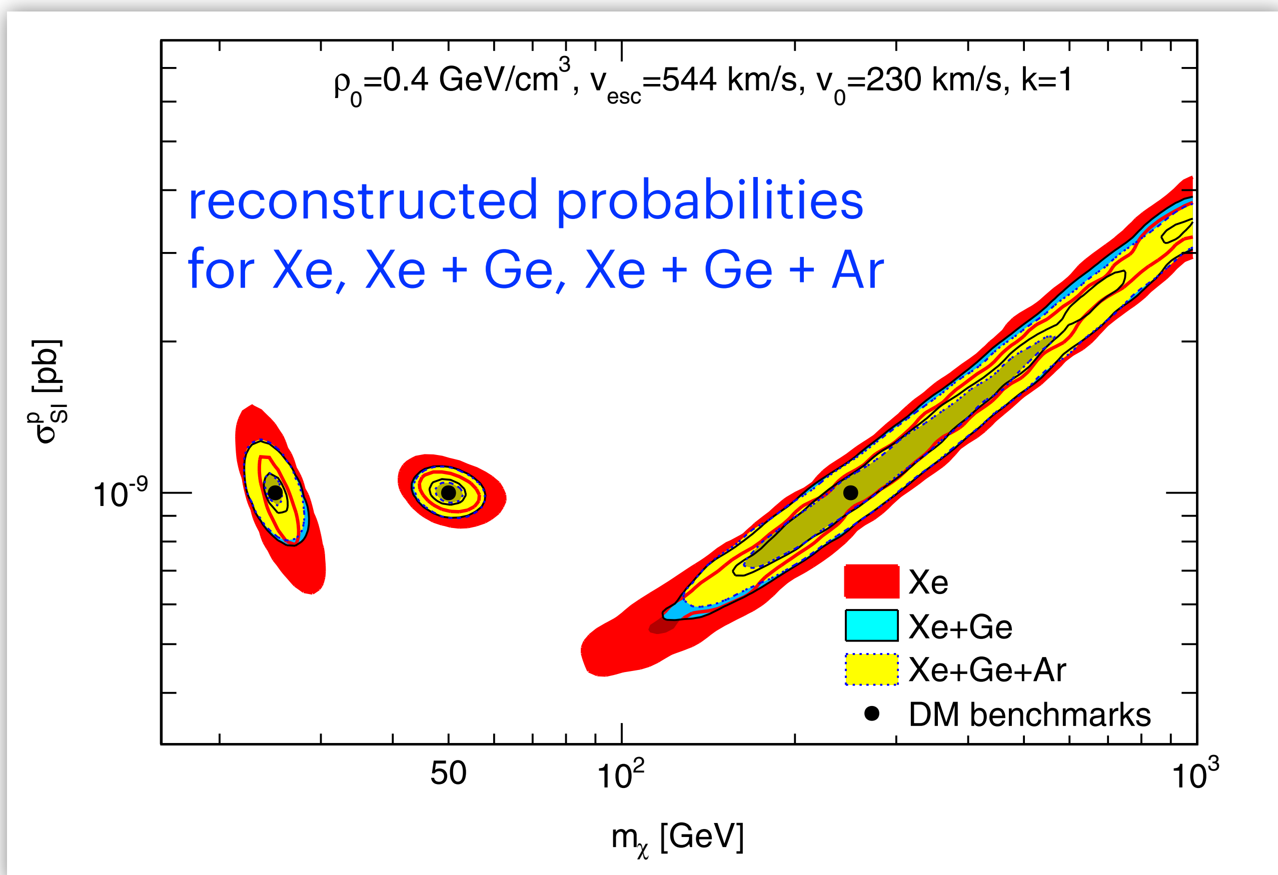

including galactic uncertainties

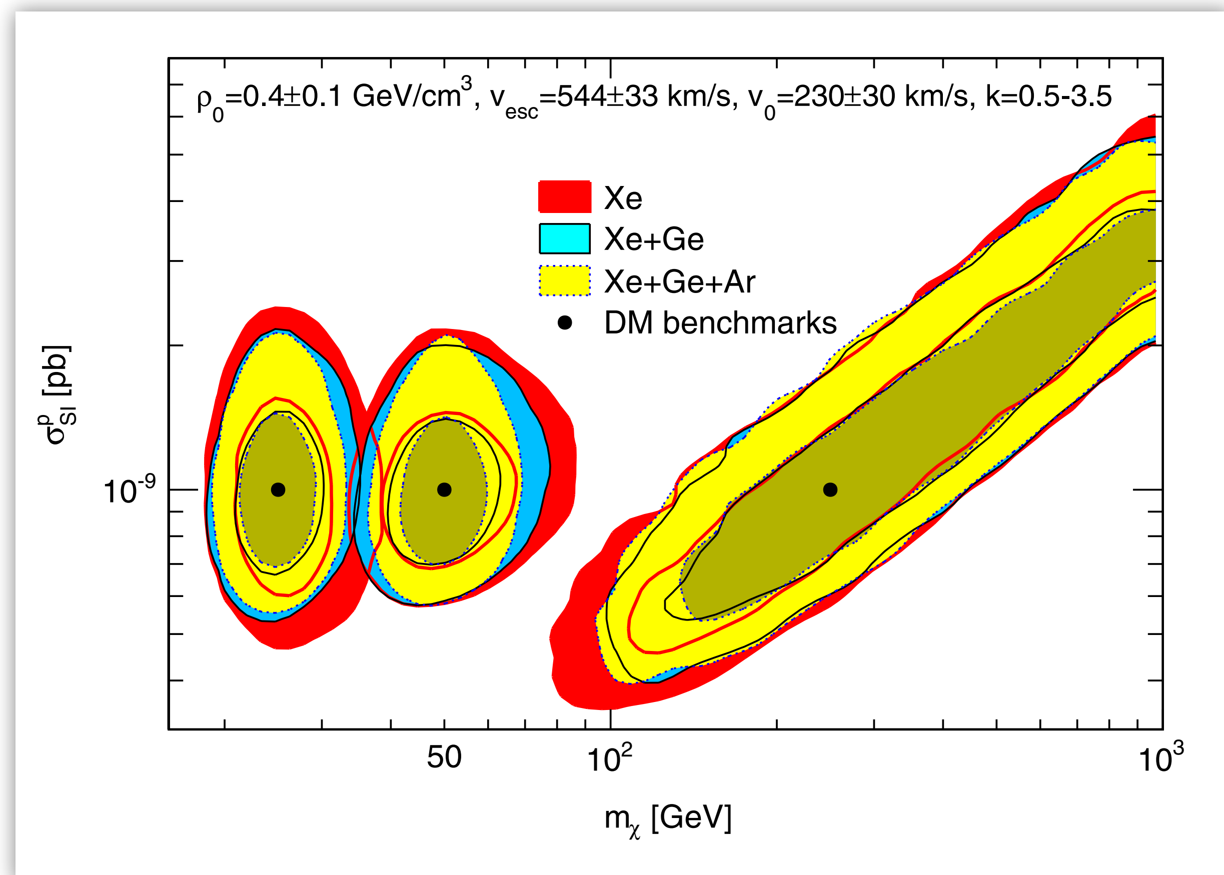

Xenon + Germanium + Argon

Pato, Baudis, Bertone, Ruiz de Austri, Strigari, Trotta: Phys. Rev. D 83, 2011

Low-mass dark matter detection

- Using the same targets as for WIMP searches, one can also search for MeV-scale and keV-scale DM
  - ◉ Interactions with electrons
  - ◉ Absorption (in the case of ALPs and dark photons)

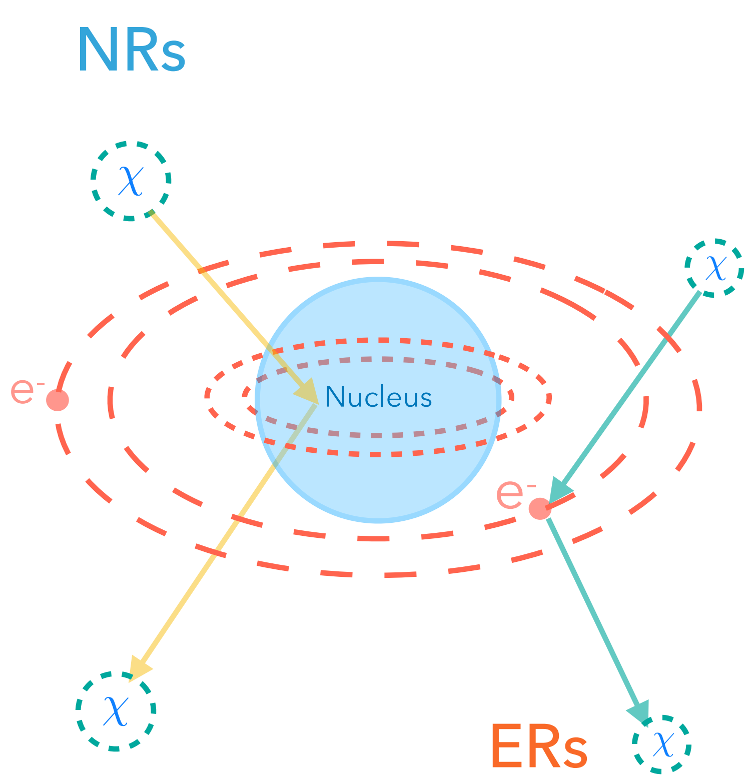

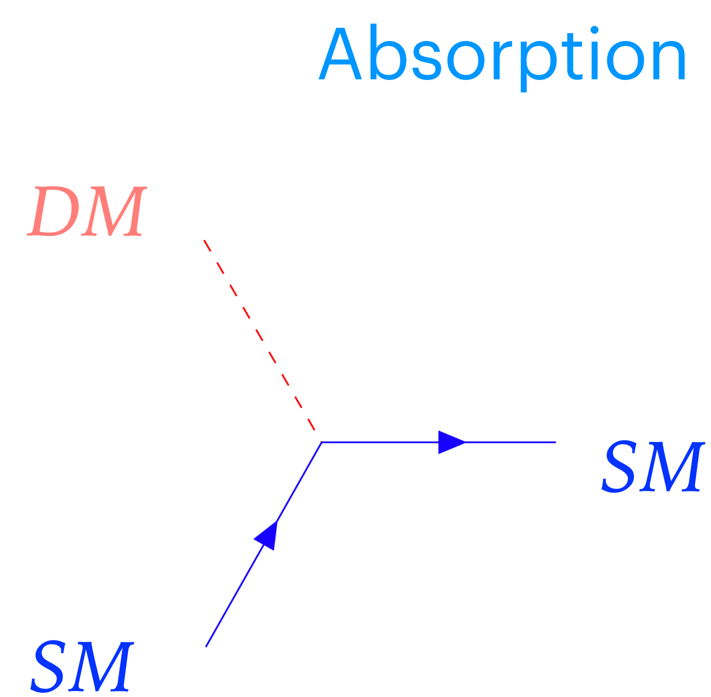

See also Tonyang Lin, Sub-GeV dark matter models and direct detection, SciPost Phys. Lect. Notes 43 (2022)

Kinematics again

- Light DM: nuclear recoil energy - well below the threshold of most experiments
- Total energy in scattering: larger, and can induce inelastic atomic processes → visible signals

$$E_e \leq \frac{m_{DM} v^2}{2} \leq 3\,\mathrm{eV} \times \frac{m_{DM}}{1\,\mathrm{MeV}}$$

$$E_{NR} = \frac{q^2}{2 m_N} \simeq 1\,\mathrm{eV} \times \left(\frac{m_{DM}}{100\,\mathrm{MeV}}\right)^2 \times \frac{10\,\mathrm{GeV}}{m_N}$$

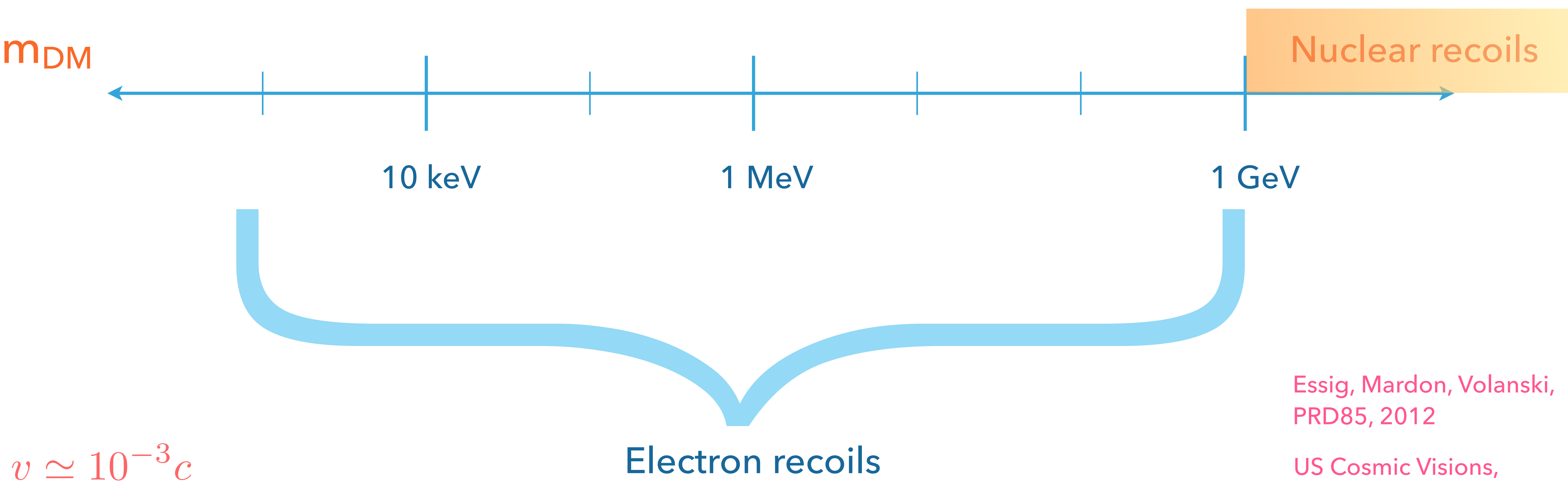

$v \simeq 10^{-3} c$

Essig, Mardon, Volanski, PRD85, 2012

US Cosmic Visions, arXiv:1707.04591

Kinematics again

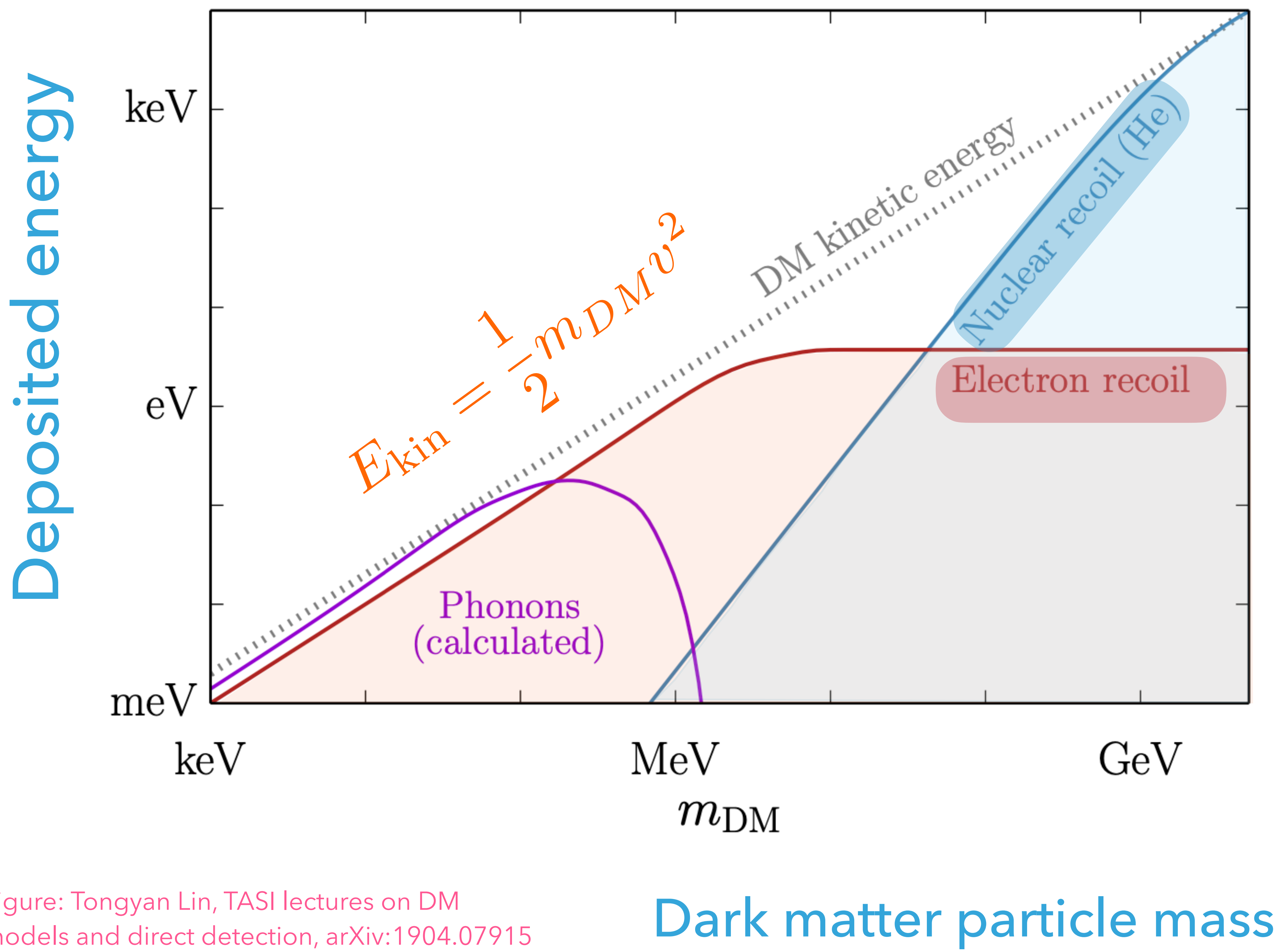

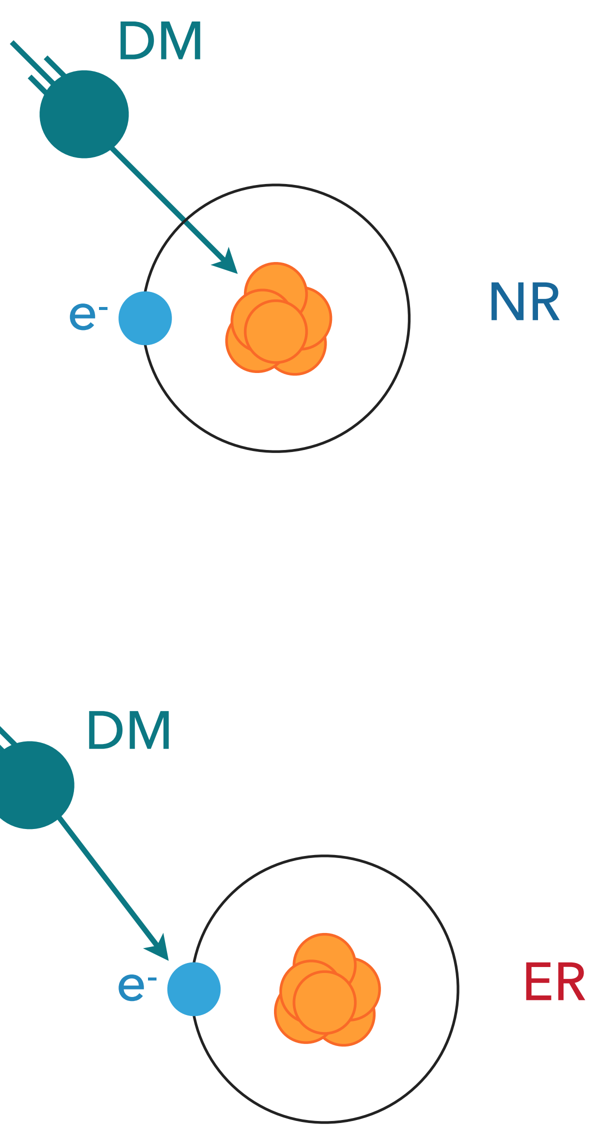

Figure: Tongyan Lin, TASI lectures on DM models and direct detection, arXiv:1904.07915

Interaction rates for DM-electron scattering

$$\frac{dR_{ion}}{d\ln E_R} = \frac{6.2}{A}\left(\frac{\rho_0}{0.4\,\mathrm{GeV\,cm^{-3}}}\right)\left(\frac{\sigma_e}{10^{-40}\mathrm{cm}^2}\right)\left(\frac{10\,\mathrm{MeV}}{m_{\mathrm{DM}}}\right)\times\frac{d\langle\sigma_{ion}v\rangle/d\ln E_R}{10^{-3}\sigma_e}\frac{\mathrm{events}}{\mathrm{kg\,d}}$$

Expected number of events for a xenon detector with 1 tonne year exposure, for 500 MeV DM mass

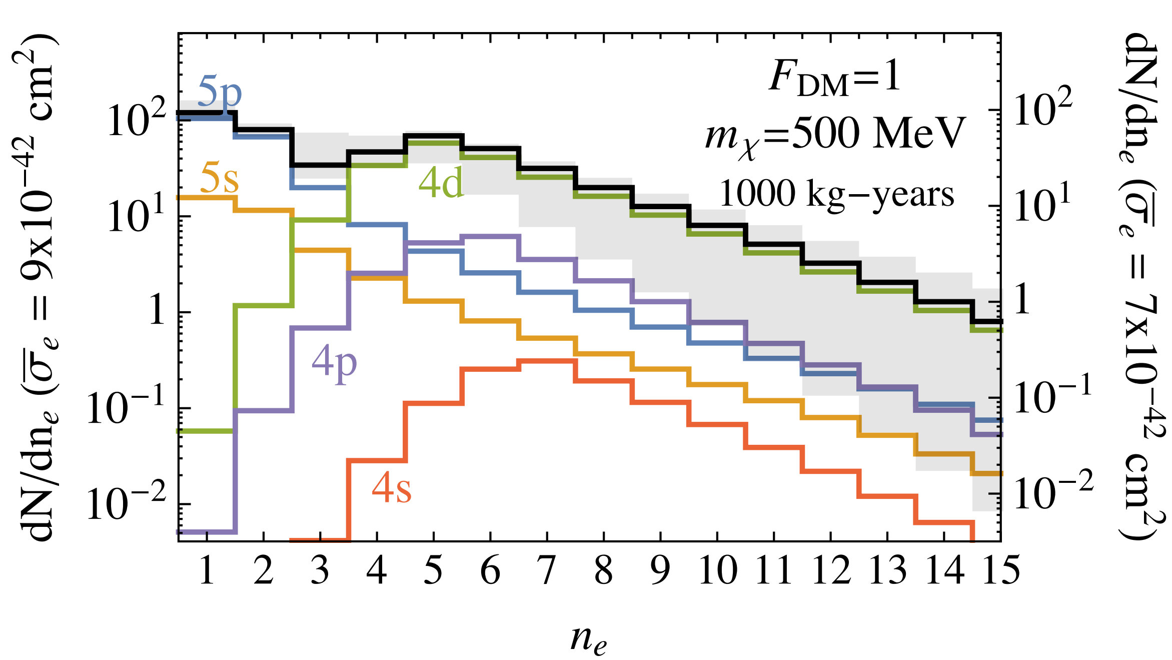

$$F_{DM} = 1$$

Heavy dark photon A' mediator

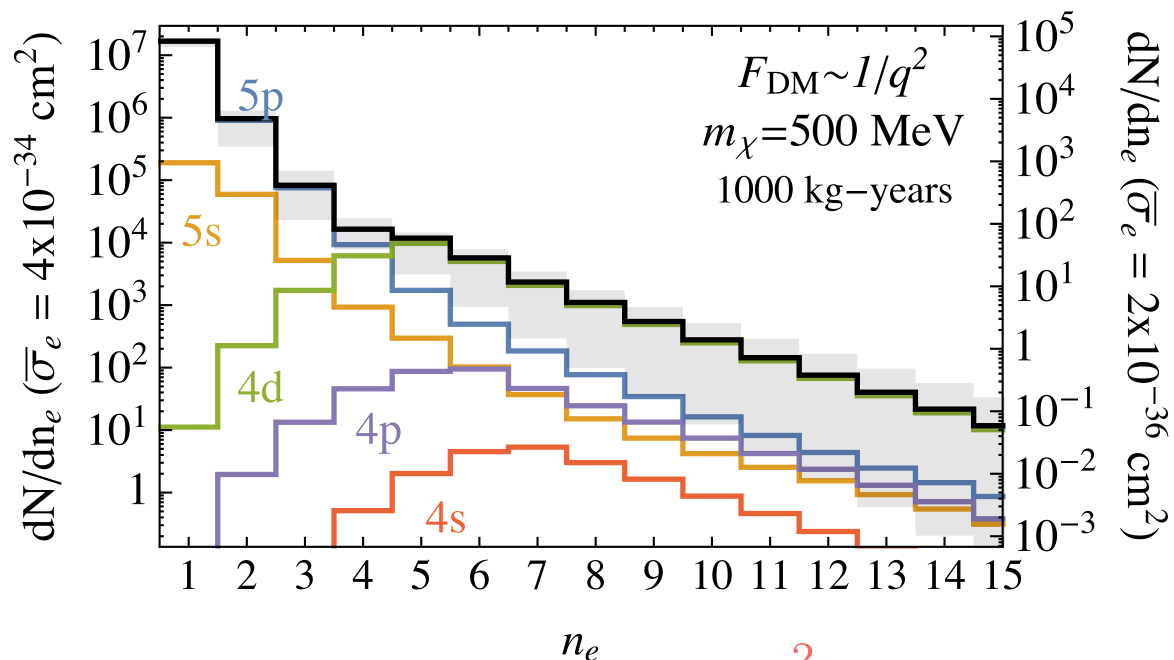

$$F_{DM} = \alpha^2\frac{m_e^2}{q^2}$$

Ultra-light dark photon A' mediator

See, e.g., Essig, Volanski, Yu, PRD 96, 2017

Interaction rates for DM absorption

- ALPs: absorption via axio-electric effect results in peak at boson mass
- Rate $\propto \phi \times \sigma = \rho \times \frac{v}{m} \times \sigma$
- for ρ = 0.3 GeV/cm^3

$$R \simeq \frac{1.5 \times 10^{19}}{A} g_{ae}^2 \left(\frac{m_a}{\mathrm{keV}}\right)\left(\frac{\sigma_{pe}}{\mathrm{b}}\right) \mathrm{kg}^{-1}\mathrm{d}^{-1}$$

$$\sigma_{ae} = \sigma_{pe} \frac{g_{ae}^2}{\beta} \frac{3E_a^2}{16\pi\alpha m_e^2}\left(1 - \frac{\beta^{2/3}}{3}\right)$$

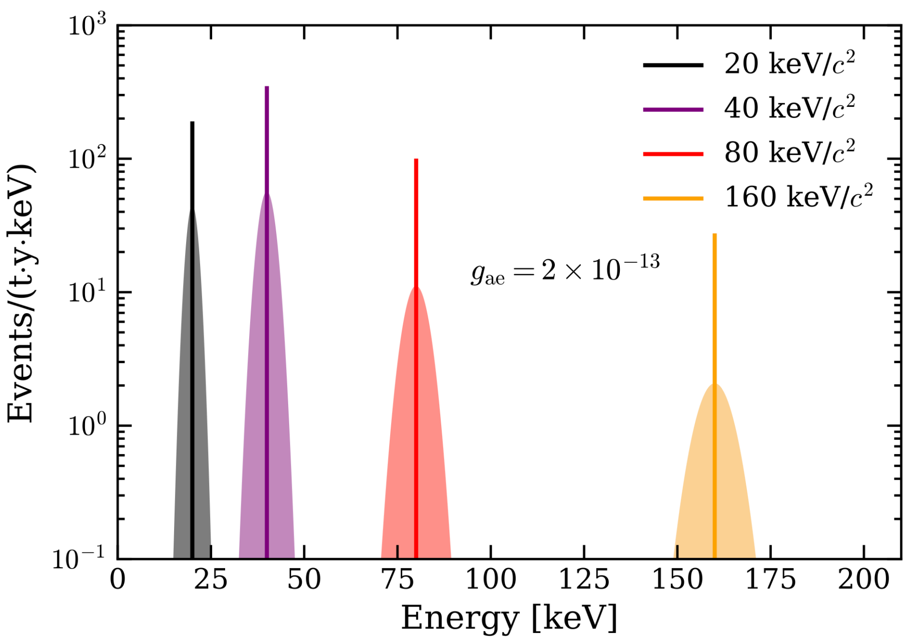

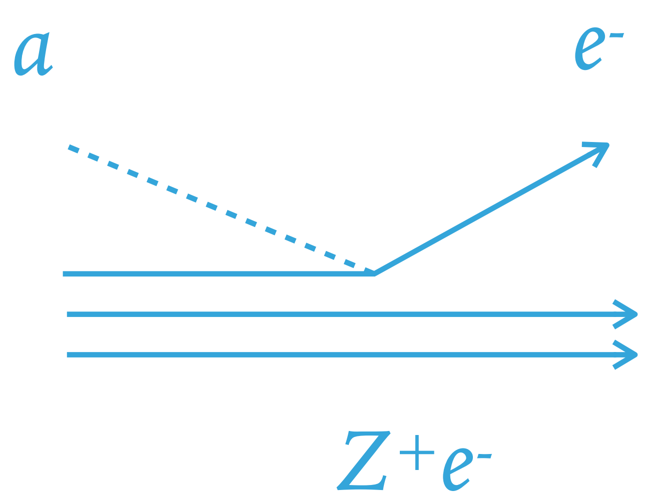

An, Pospelov, Pradler, Ritz PLB 747, 2015

Interaction rates for DM absorption

- Dark photons: absorption results in peak at boson mass
- Rates $\propto \phi \times \sigma = \rho \times \frac{v}{m} \times \sigma$
  - for ρ = 0.3 GeV/cm^3

$$R \simeq \frac{4.7 \times 10^{23}}{A} \kappa^2 \left(\frac{\mathrm{keV}}{m_V} \right) \left(\frac{\sigma_{pe}}{\mathrm{b}} \right) \mathrm{kg}^{-1} \mathrm{d}^{-1}$$

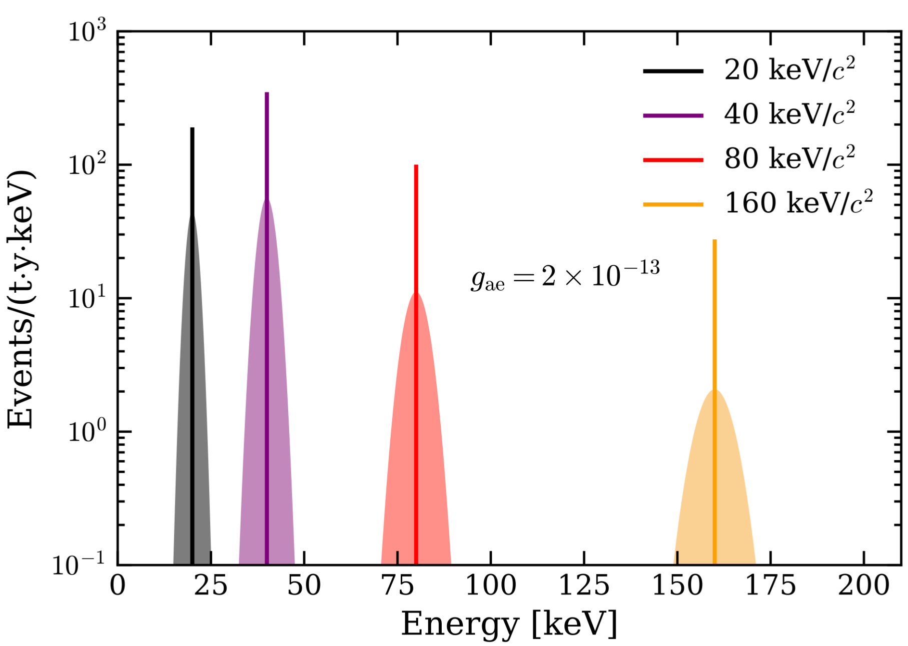

$$\sigma_v \simeq \frac{\sigma_{pe}}{\beta} \kappa^2$$

strength of kinetic mixing between photon and dark photon

An, Pospelov, Pradler, Ritz PLB 747, 2015

Examples: constraints on LDM interactions

XENON, PRD 106, 022001 (2022)

DM-electron scatters

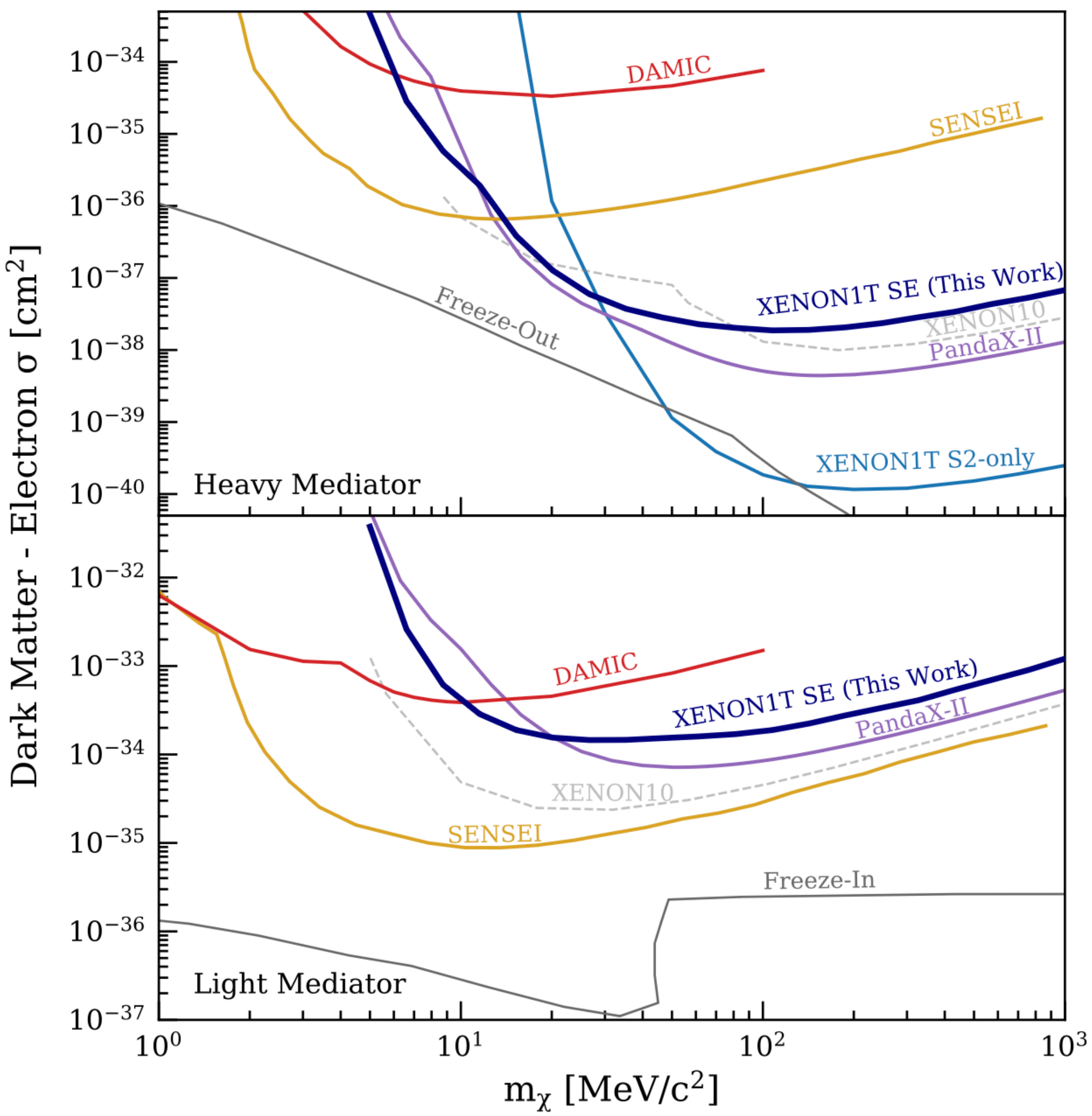

Dark photons and ALPs absorption

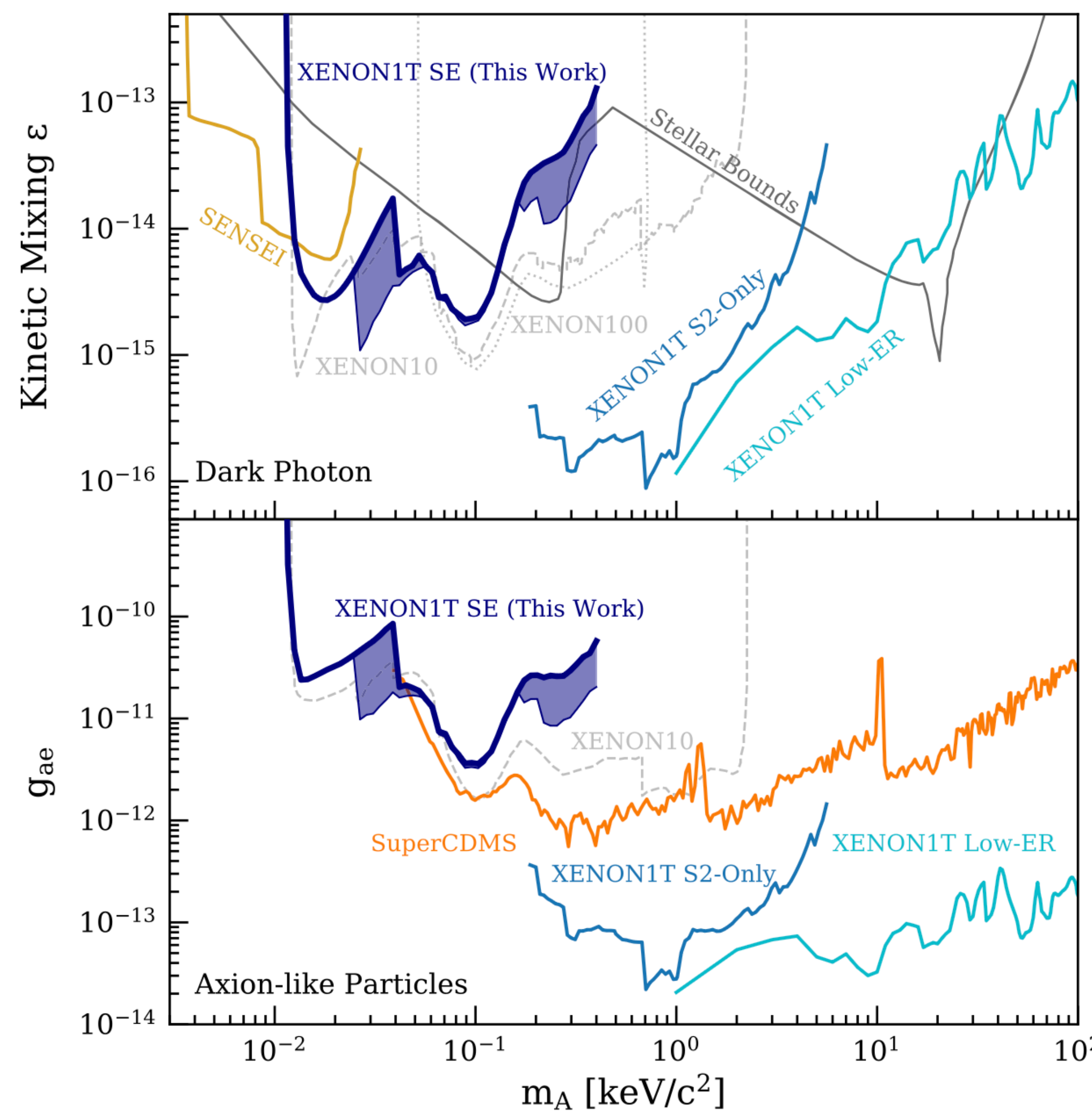

DM-mass: 1 MeV - 1 GeV

DM-mass: few eV - 100 keV

End of Lecture 1